# Co based multilayer systems for controllable domain wall positioning

M. Urbaniak

F. Stobiecki
B. Szymański
A. Jarosz
P. Kuświk
M. Matczak
M. Schmidt
J. Aleksiejew

A. Ehresmann
A. Gaul

Institute of Molecular Physics
Polish Academy of Sciences
POZNAŃ

University of
KASSEL

# Co based multilayer systems for controllable domain wall positioning

## OUTLINE

- Introduction
- Perpendicular magnetic anisotropy in Co based multilayers
- Properties modification by ion bombardment
- Domain wall control with anisotropy gradient
- Domain wall control with coupling gradient

# Potential uses of controllable wall positioning

- magnetic memories – race track memory, S.S.P. Parkin, IBM

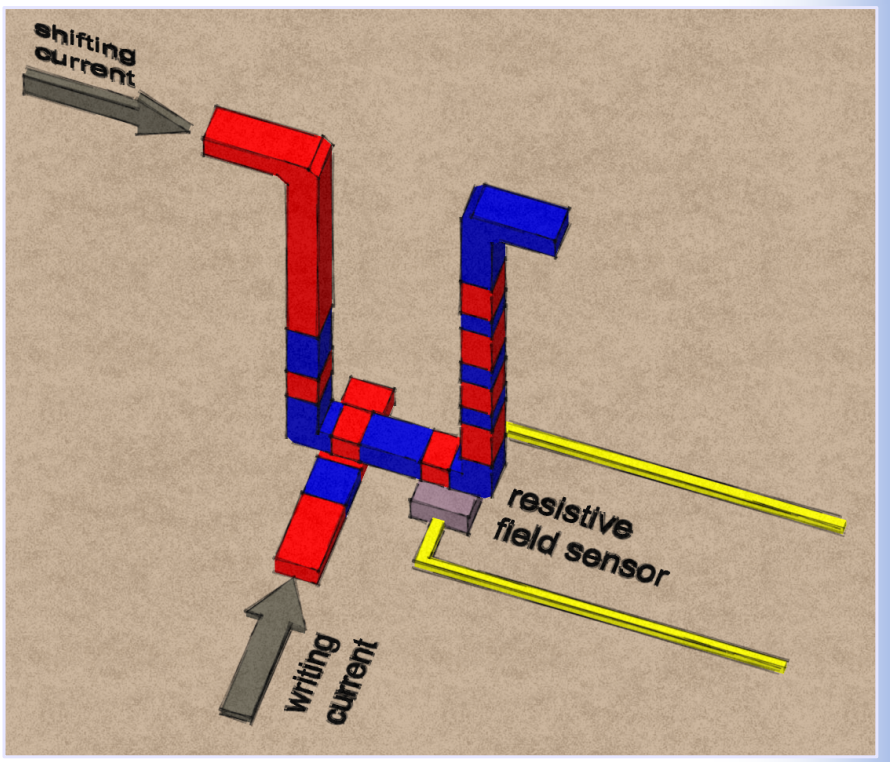


- magnetic field sensors with memory – resistance depends on domain wall position, IFM PAN

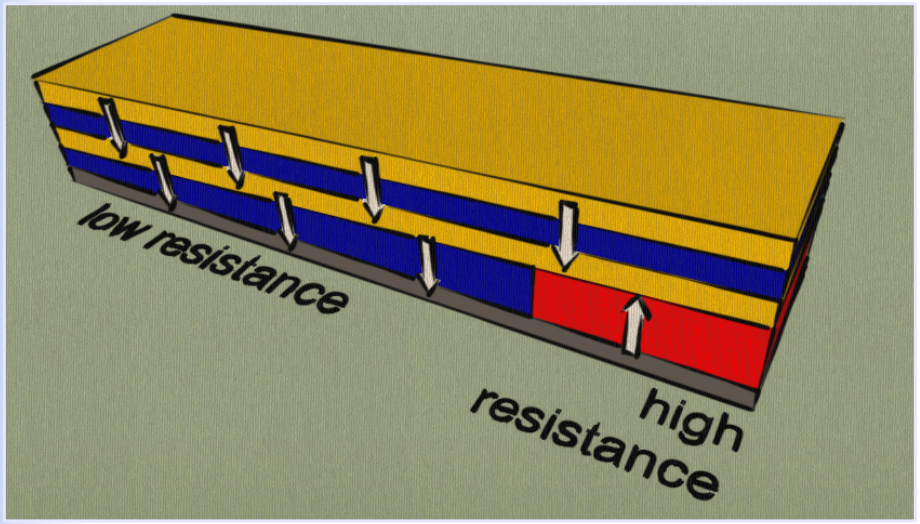


- magnetophoresis of magnetic beads: lab-on-chip devices using functionalized beads

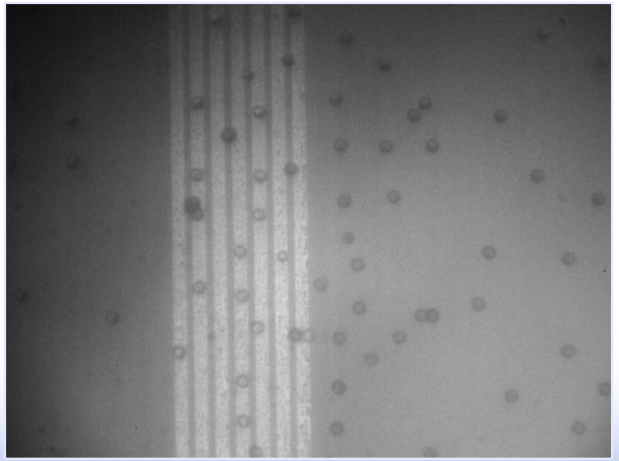

- the nucleation of walls often requires much higher fields than those required to sustain the domain wall motion
- if one measures the hysteresis keeping the rate of change of magnetization very slow the so called ***reentrant loop*** can be obtained [1,3]

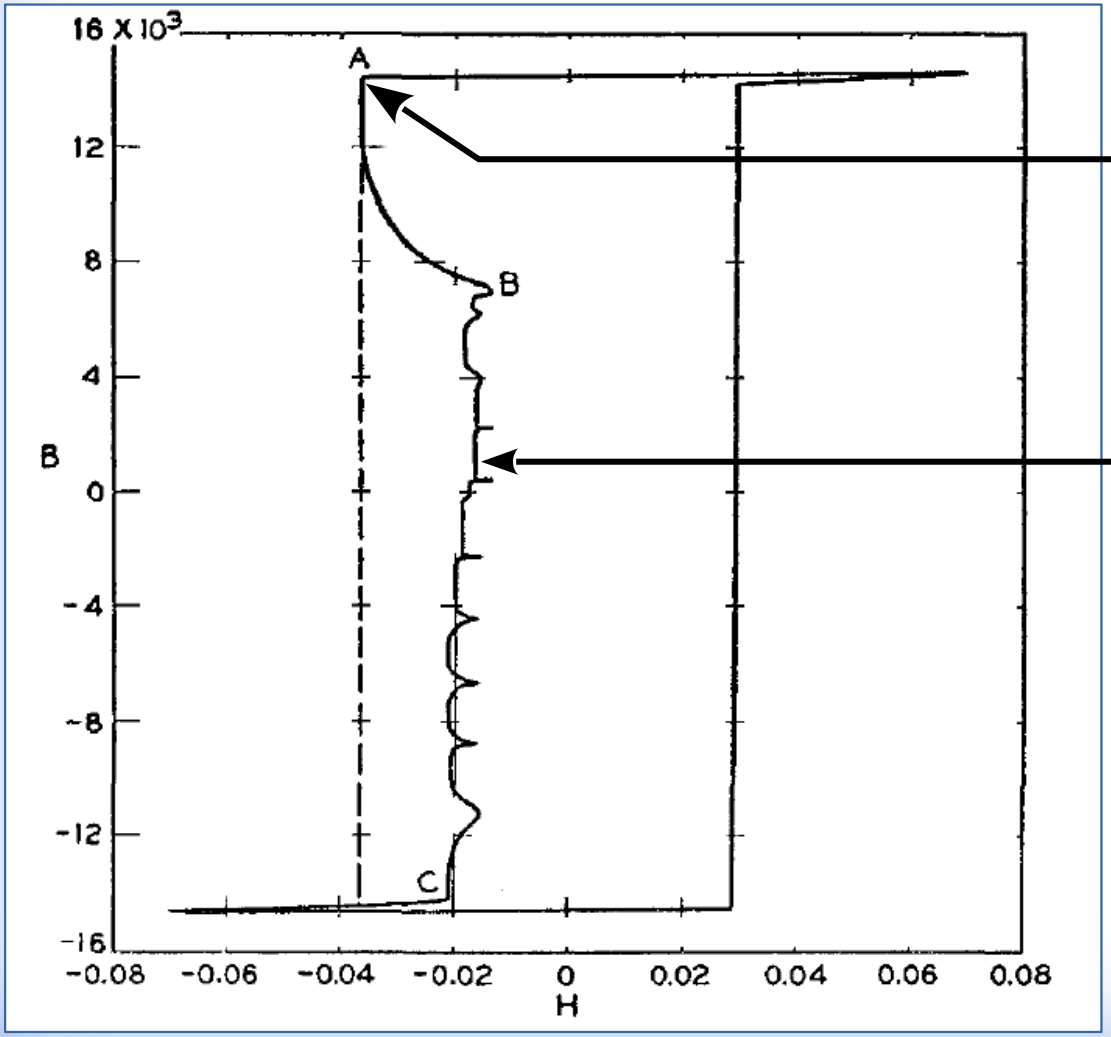


domain walls start to move

weaker field is sufficient to sustain wall motion

Hysteresis loop of Perminvar after magnetic anneal. **A -Starting field**; A -B-rapid decrease of applied field; **B-C-traced under equilibrium conditions**. Dotted line indicates path described if field had not been reduced to critical field.

Perminvar (Ni 45%, Fe 30%, Co 25%)

H. J. Williams and Matilda Goertz, J. Appl. Phys. 23, 316 (1952)

- after switching the external field off the systems moves to the nearest energy minimum
- in bulk samples the position of minimum is not controllable
- in patterned structures the position corresponding to the minimum can be set with the geometry

Since **automotive DW motion always occurs toward the narrowest part of ring,...**

Py, 30nm

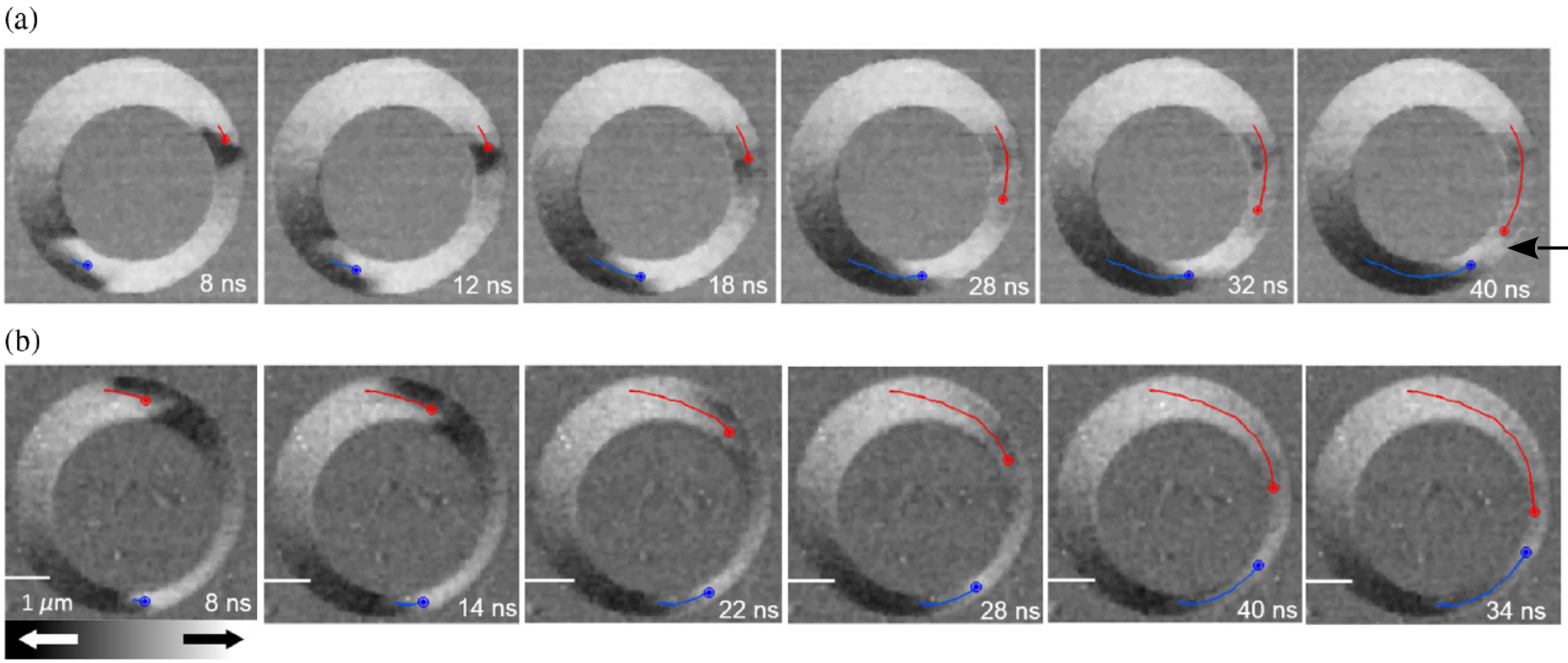


FIG. 3. Time-resolved STXM XMCD snapshots of automotive DWs' motion during the switching process from the onion to the vortex state in the ferromagnetic rings for the case of equal (a) and opposite (b) vortex wall chirality. These snapshots represent part of the XMCD videos used to extract the DW velocities plotted in Fig. 2. Red and blue lines illustrate the averaged trajectory of the vortex core of both vortex walls head to head and tail to tail, respectively.

image from: M-A. Mawass et al., Physical Review Applied 7, 044009 (2017)

the tendency of the domain walls to minimize its length – the neck acts as a pinning center

NiFe(20 nm)/Cu(10 nm)/NiFe(5 nm)

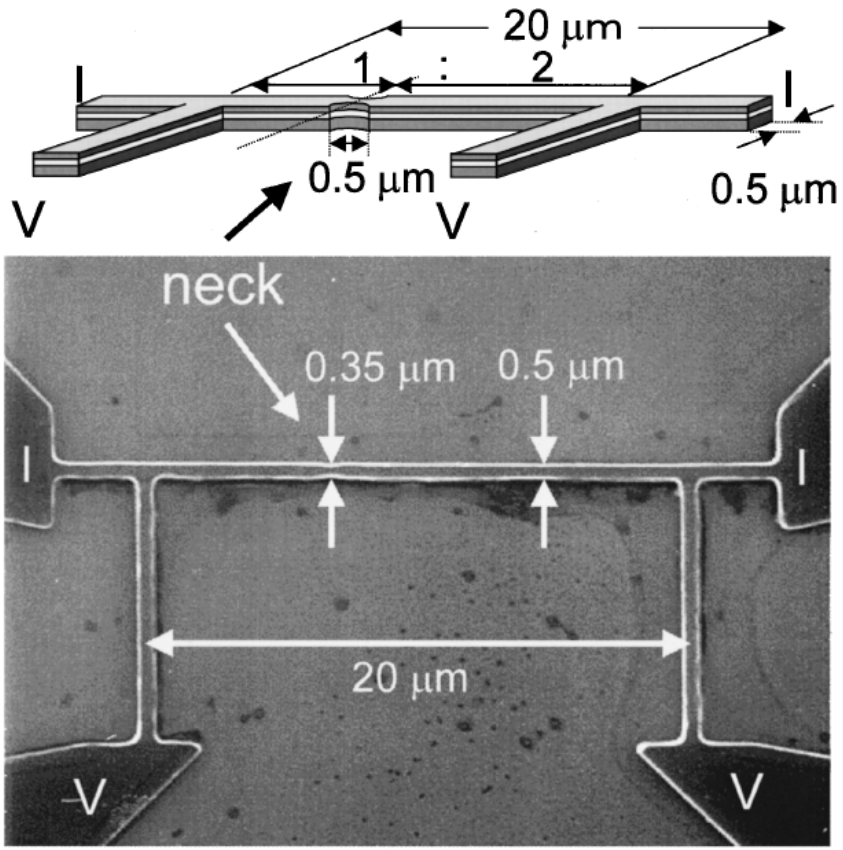


FIG. 1. SEM image and schematic illustration of the sample. The sample consists of a NiFe(200 Å)/Cu(100 Å)/NiFe(50 Å) trilayer.

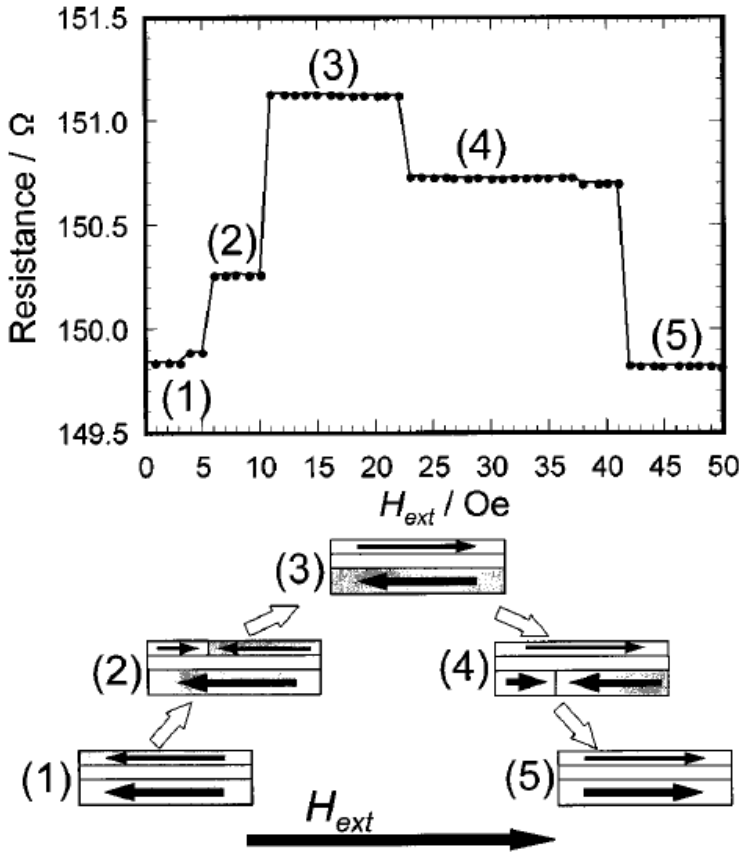


FIG. 2. Resistance as a function of the external magnetic field at 300 K determined by the four-point dc technique as illustrated in Fig. 1. The magnetic domain structures inferred from the resistance measurement and the direction of the external field are schematically shown.

T. Ono, H. Miyajima, K. Shigeto, and T. Shinjo, Appl. Phys. Lett. **72**, 1116 (1998)

Some ways to control the position of a domain wall:

- move your sample :)
- use geometrical constraints
- use gradient of properties to change switching fields:
  - temperature gradient
  - stress gradient
  - thickness gradient
  - anisotropy gradient
  - coupling gradient

Some ways to control the position of a domain wall:

- move your sample :)
- use geometrical constraints
- use gradient of properties to change switching fields:
  - temperature gradient
  - stress gradient
  - thickness gradient
  - **anisotropy gradient**
  - **coupling gradient**

# Perpendicular magnetic anisotropy in Co based multilayers

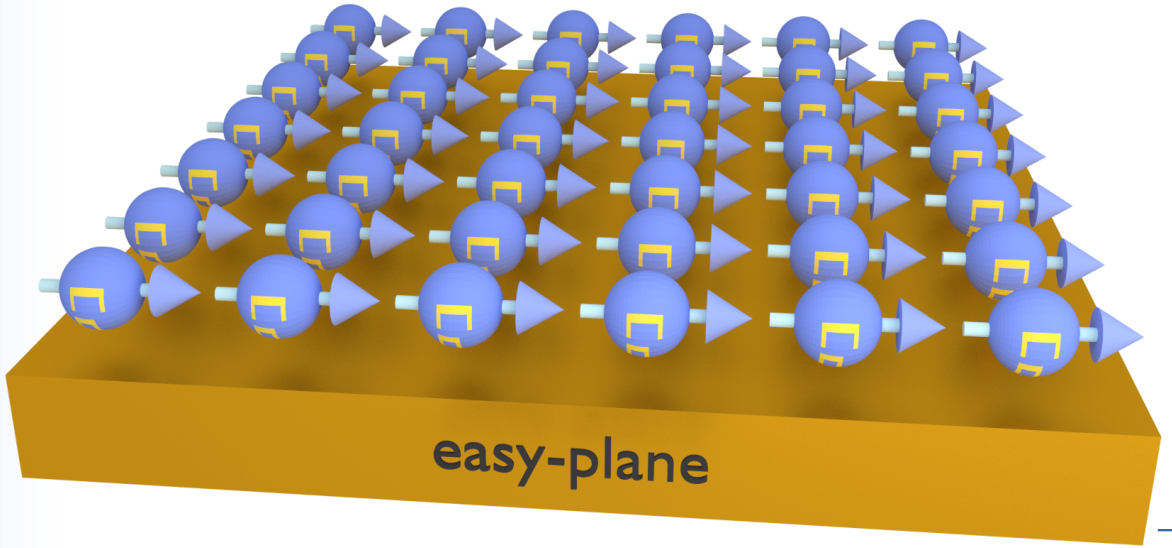


Due to the shape anisotropy thin ferromagnetic layer possess usually the anisotropy which favors in-plane orientation of magnetic moments

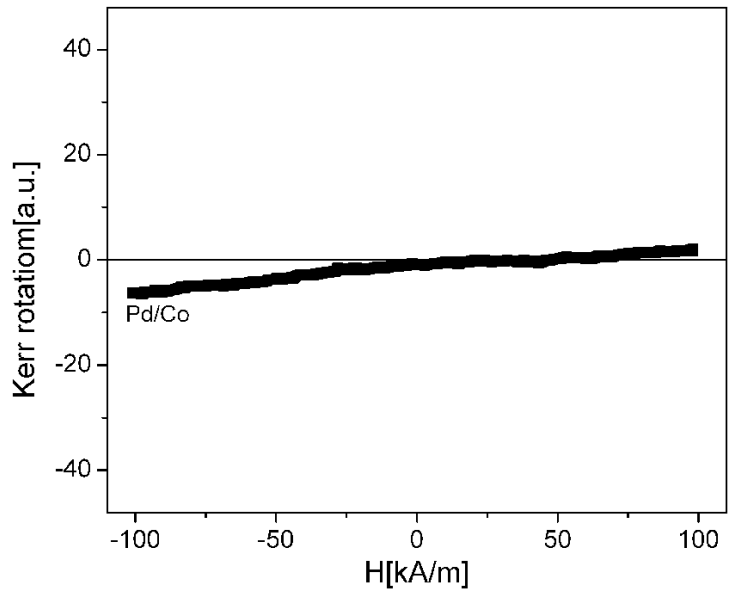

# Perpendicular magnetic anisotropy in Co based multilayers

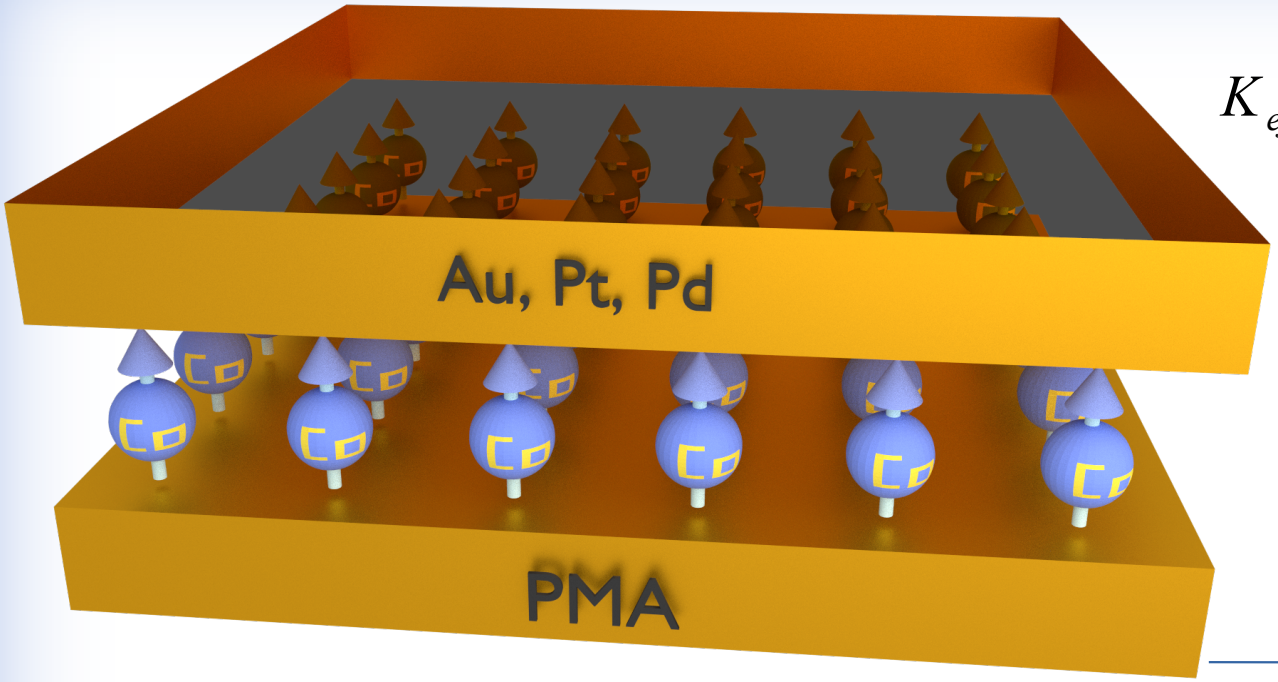


$$K_{eff} = \frac{2K_{1s}}{t_{Co}} + K_{1v} - \frac{1}{2}\mu_0 \left(M_S^{Co}\right)^2$$

Co based multilayers in which magnetic layer is sandwiched between noble metal spacer possess perpendicular magnetic anisotropy (PMA) in limited thickness range – this is due to **surface anisotropy** of the interfaces

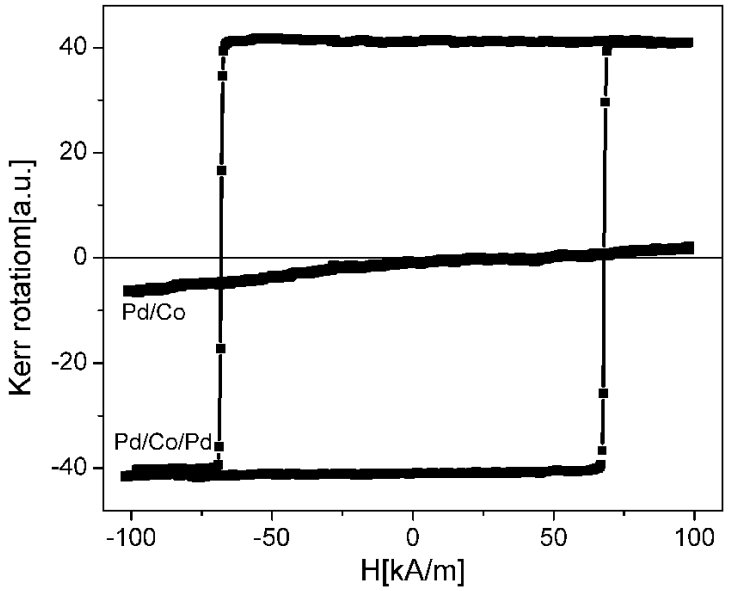


*for Co/Au MLs the PMA range is approximately 0.5-1.2nm

# Perpendicular magnetic anisotropy in Co based multilayers

Co based multilayers in which magnetic layer is sandwiched between noble metal spacer possess perpendicular magnetic anisotropy (PMA) in limited thickness range – this is due to **surface anisotropy** of the interfaces

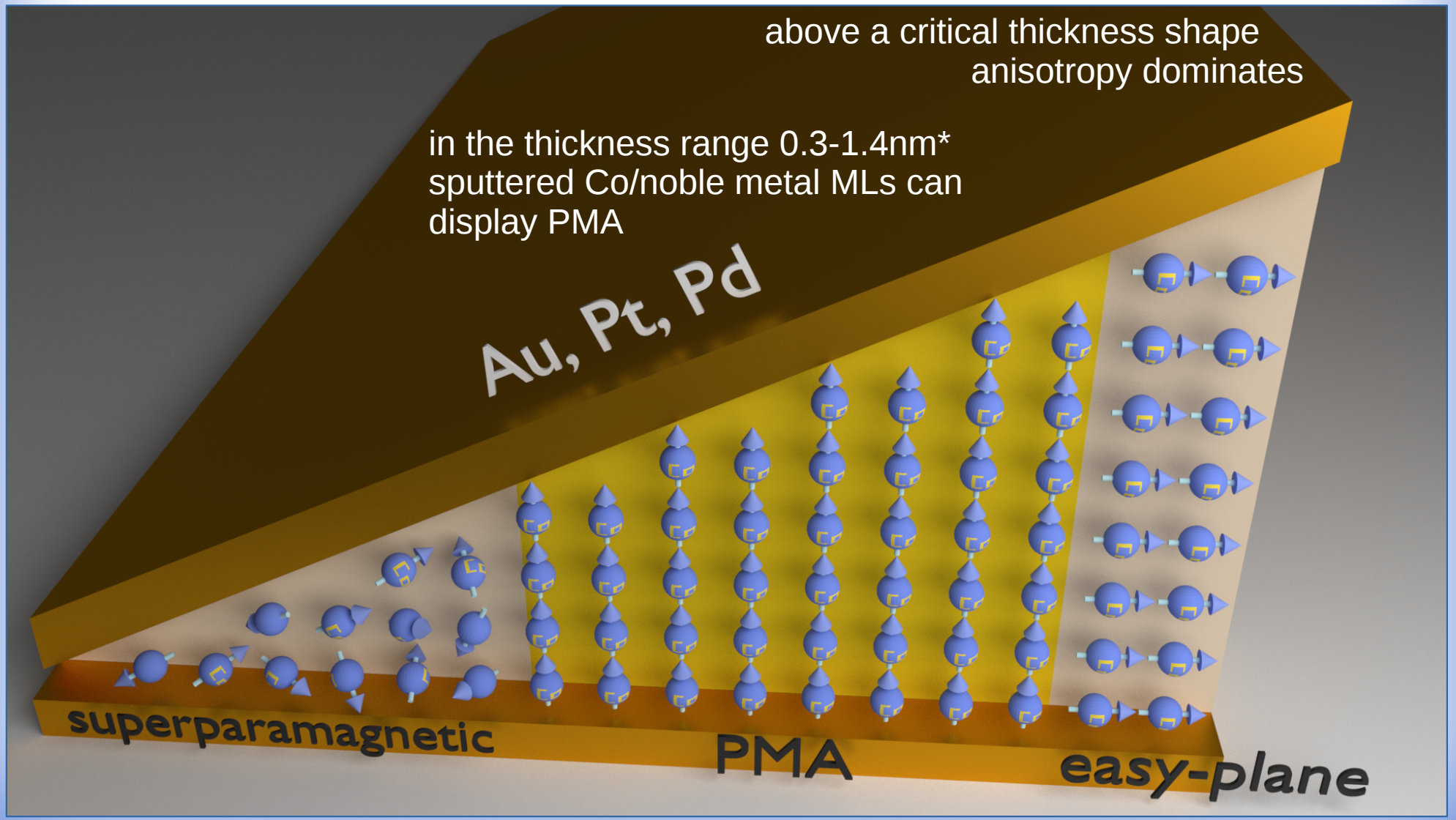


*for Co/Au MLs the PMA range is approximately 0.5-1.2nm

Co based multilayers in which magnetic layer is sandwiched between noble metal spacer possess perpendicular magnetic anisotropy (PMA) in limited thickness range – this is due to **surface anisotropy** of the interfaces

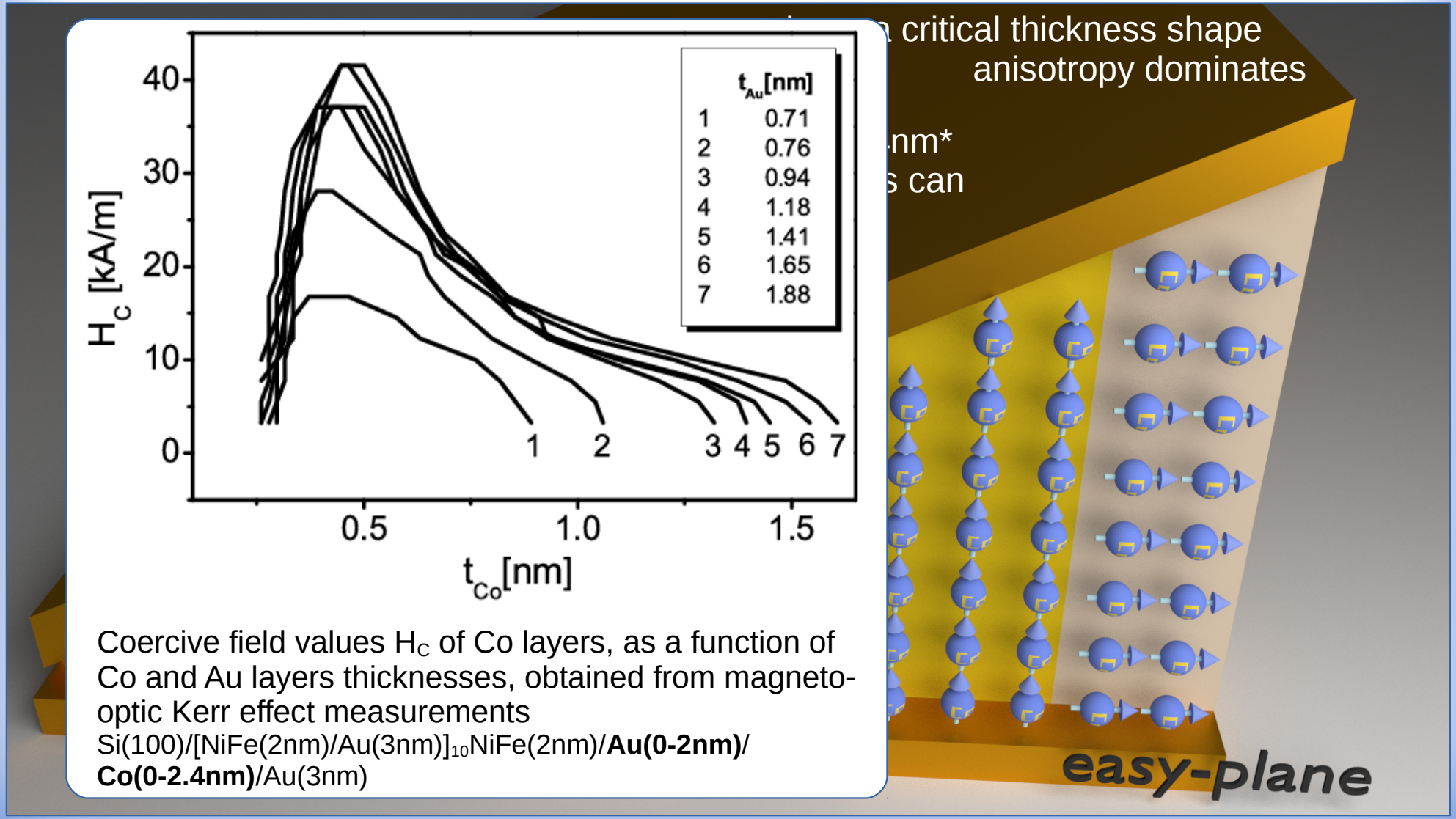





Coercive field values $H_C$ of Co layers, as a function of Co and Au layers thicknesses, obtained from magneto-optic Kerr effect measurements

Si(100)/[NiFe(2nm)/Au(3nm)]$_{10}$NiFe(2nm)/**Au(0-2nm)**/**Co(0-2.4nm)**/Au(3nm)

*for Co/Au MLs the PMA range is approximately 0.5-1.2nm

- as-deposited Si(100)/Au/[Co(0.8nm)/Au(1nm)]$_2$
- perpendicular magnetic anisotropy
- remanence Kerr microscopy **difference images**

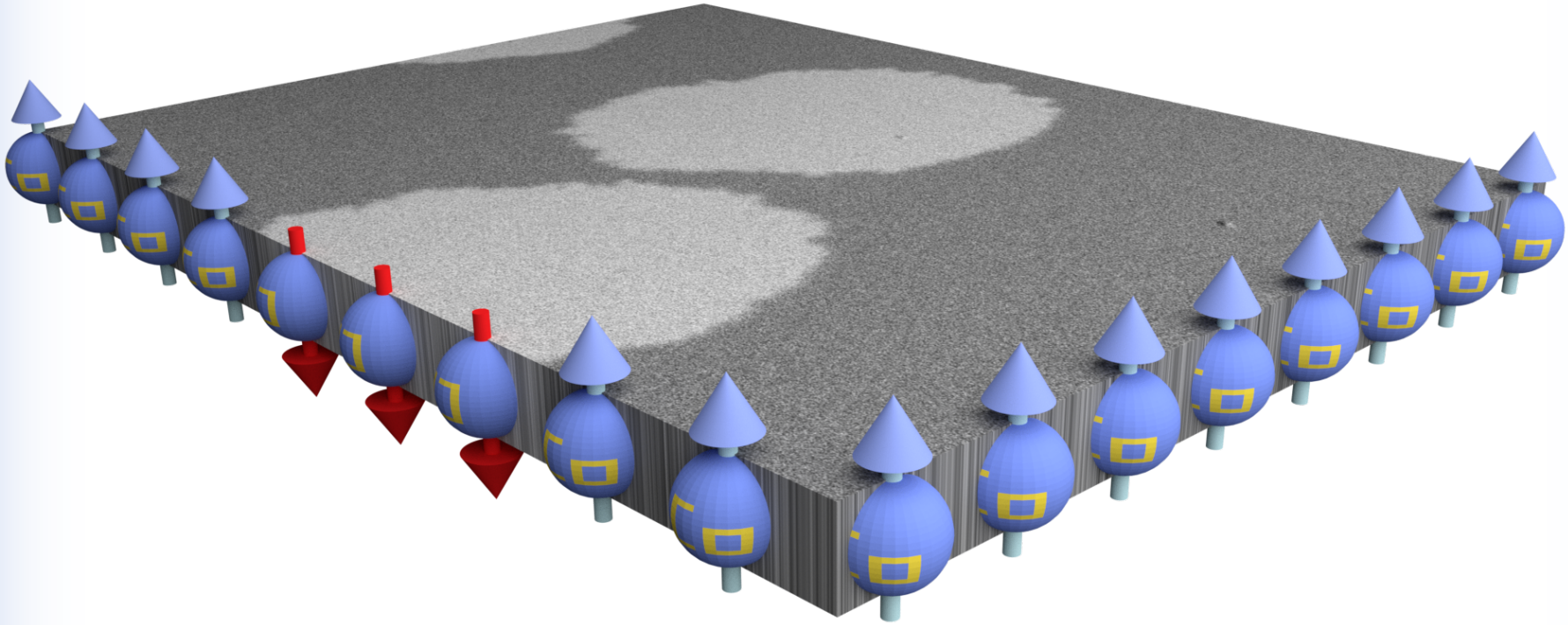

small number of repetitions – no stripe domains

Co based multilayers in which magnetic layer is sandwiched between noble metal spacer possess perpendicular magnetic anisotropy (PMA) in limited thickness range – this is due to **surface anisotropy** of the interfaces

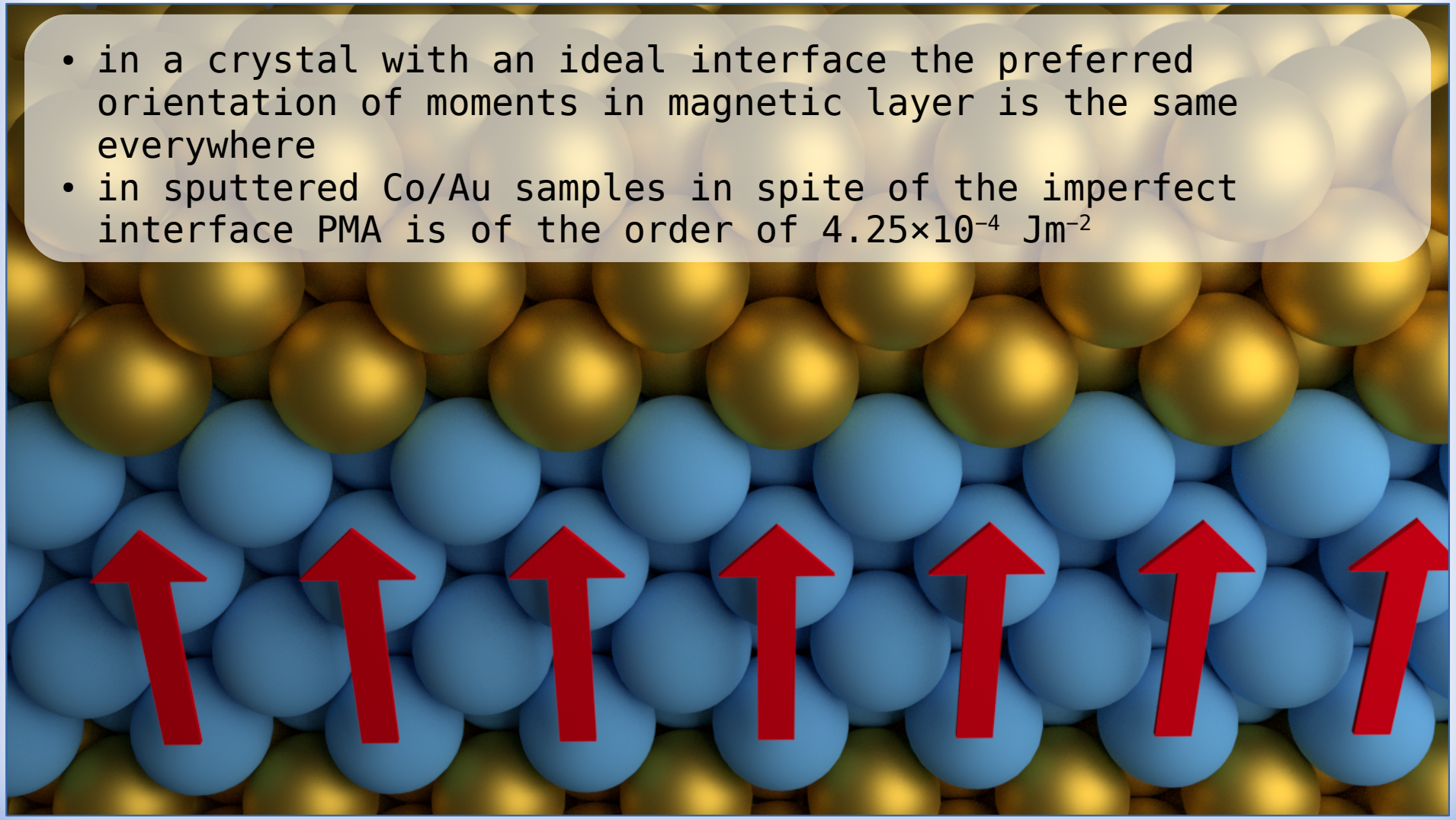

Co based multilayers in which magnetic layer is sandwiched between noble metal spacer possess perpendicular magnetic anisotropy (PMA) in limited thickness range – this is due to **surface anisotropy** of the interfaces

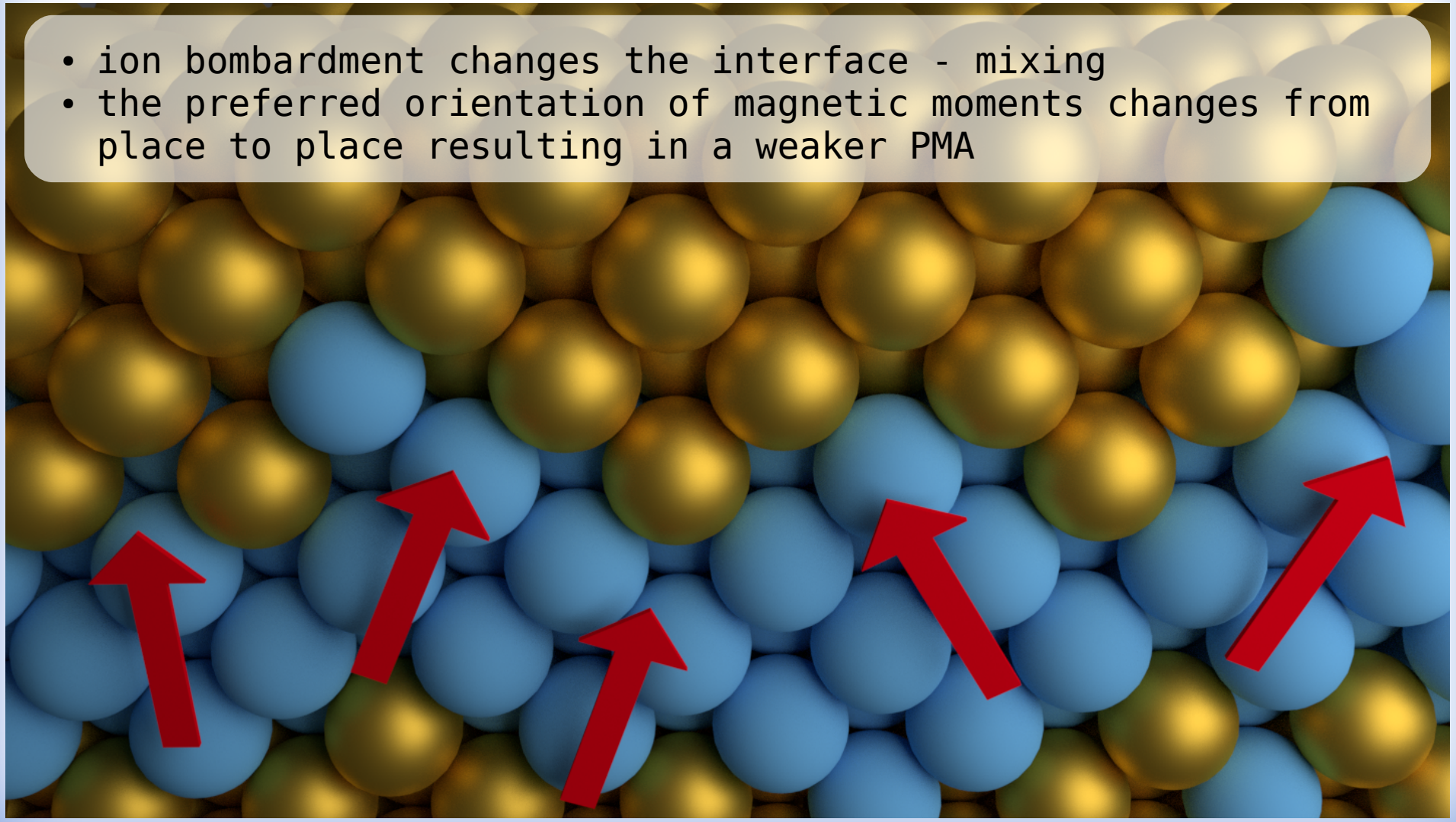

The influence of the ion bombardment:

- moderate fluences can be used to modify the switching fields
- higher fluences, depending on the Co layer thickness, lead either to a change to an easy-plane anisotropy or destroy ferromagnetic order

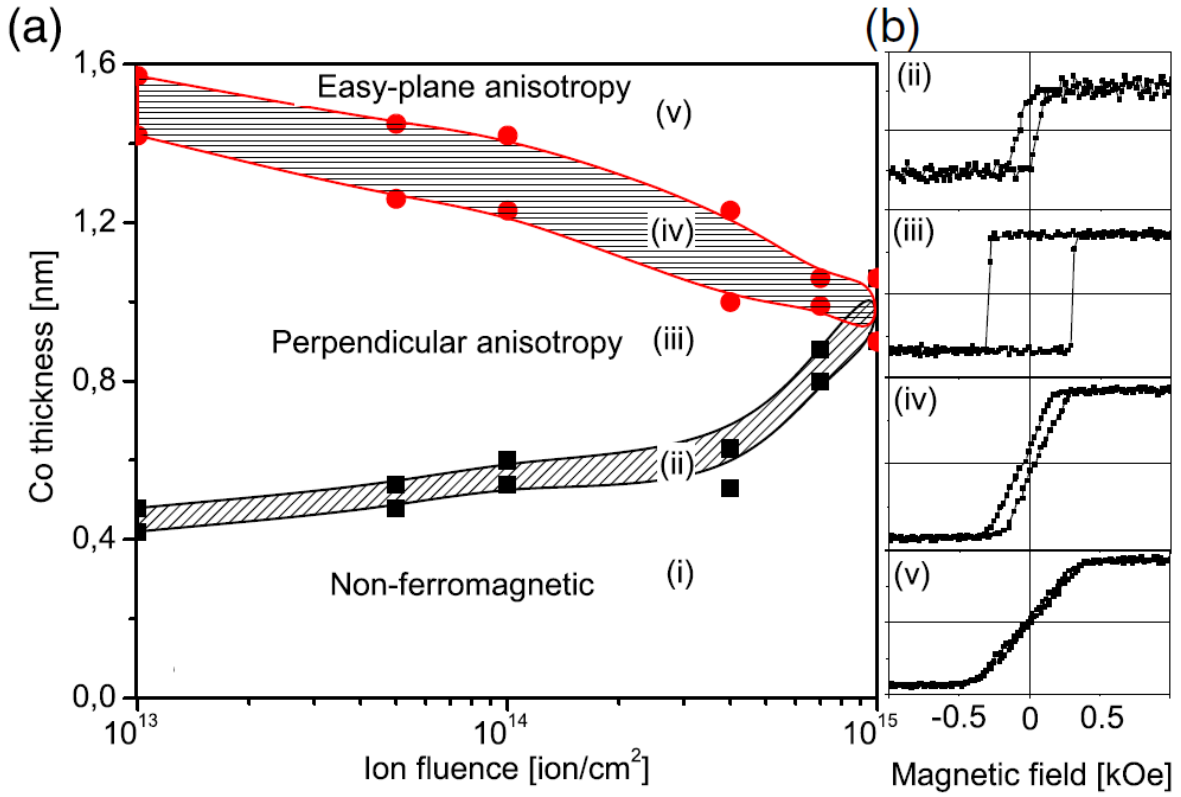


10 keV $He^+$

**Figure 3.** Magnetic phase changes of the Co layer as a function of Co layer thickness caused by bombardment with 10 keV $He^+$ ions. (a) Variation of the Co thickness intervals (i)–(v) as a function of $He^+$ ion fluence. (b) Hysteresis loops corresponding to thickness intervals (ii)–(v). Dashed areas (ii) and (iv) are guides to the eye for the transition regimes.



P. Kuświk et al., Nanotechnology **22**, 095302 (2011)

# Domain wall propagation driven reversal in $(Co/Au)_2$ films

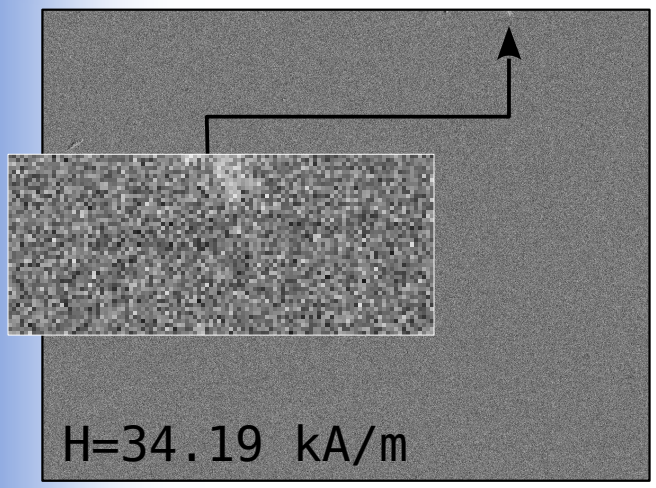


approx. 895×687 μm²

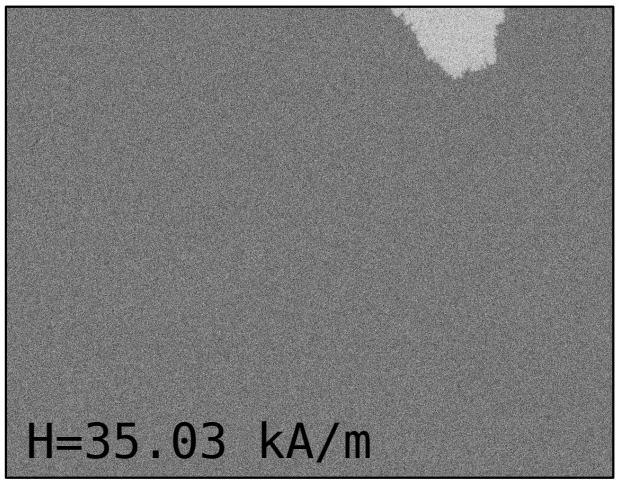


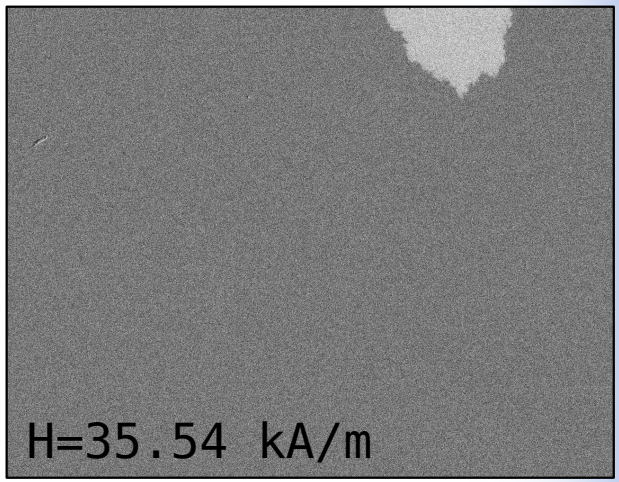


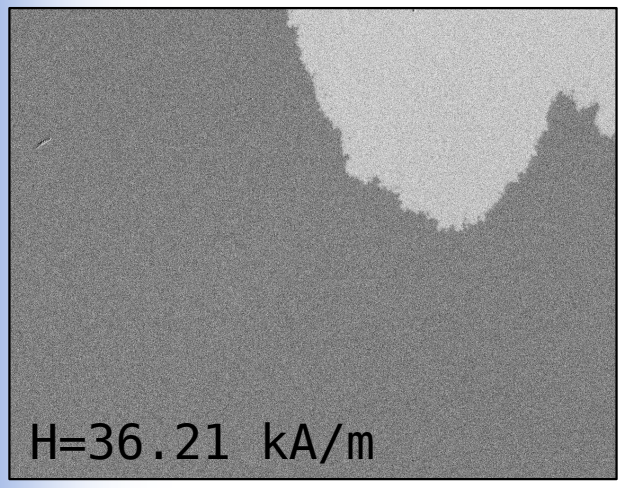


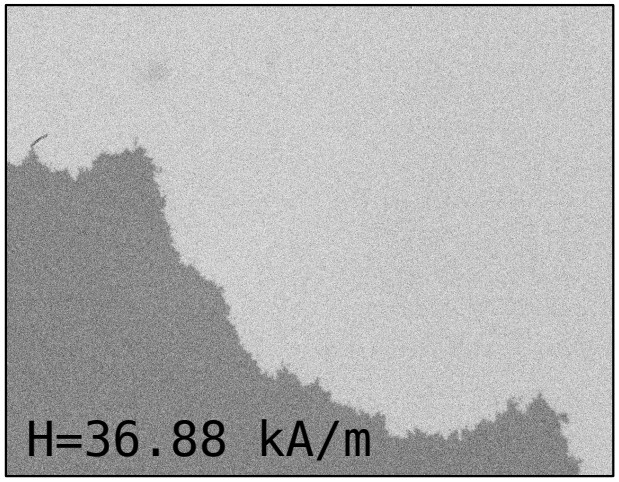


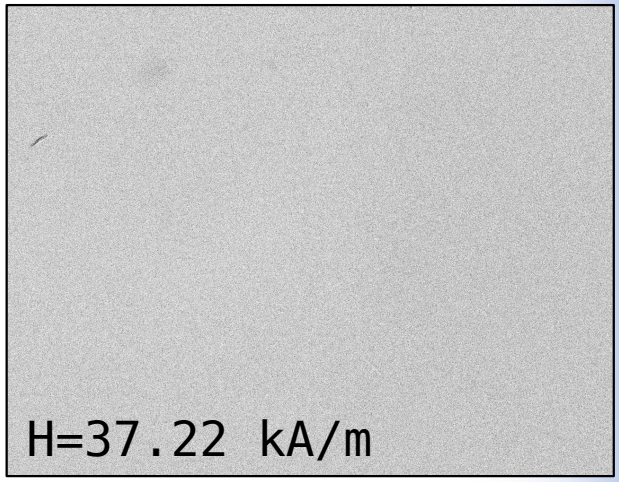


In films deposited by sputtering the density of nucleation centers can be very low. For the series of images shown above there seems to be no nucleation center within the image (approx. 0.9 x 0.7 mm²)

Domain wall propagation driven reversal in $(Co/Au)_2$ films

- **randomly distributed nucleation centers**
- **no control over the nucleation**

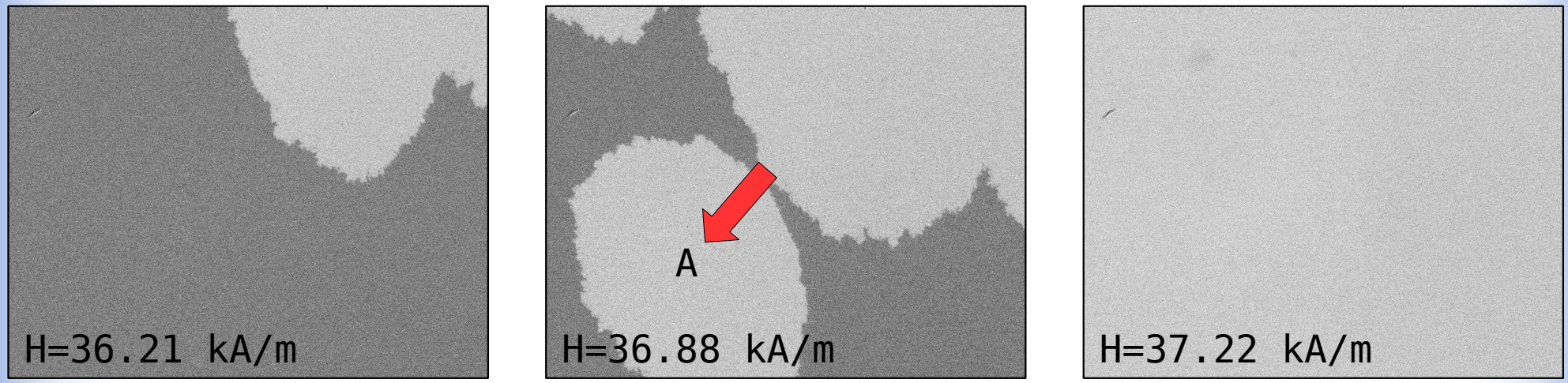


The exact evolution of the domains is not reproducible as evidenced by a domain expanding from the probable nucleation center near the point A.

# Nucleation centers

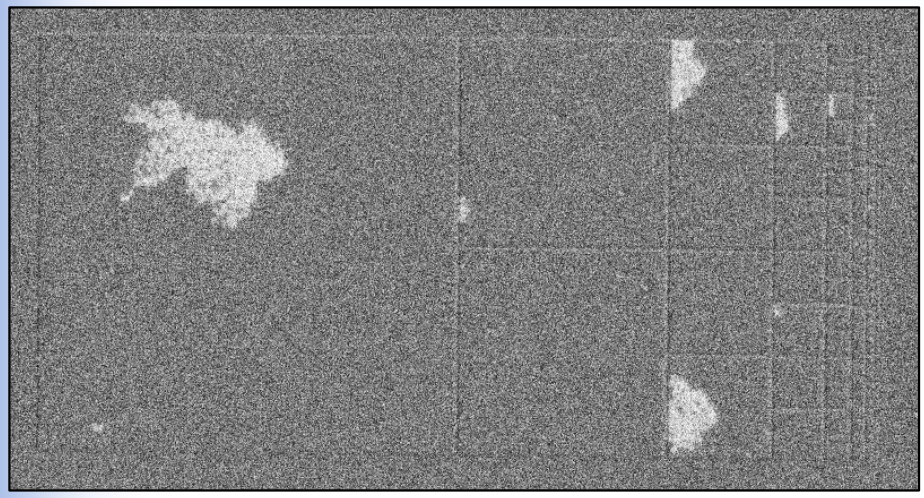

H=34.7 kA/m

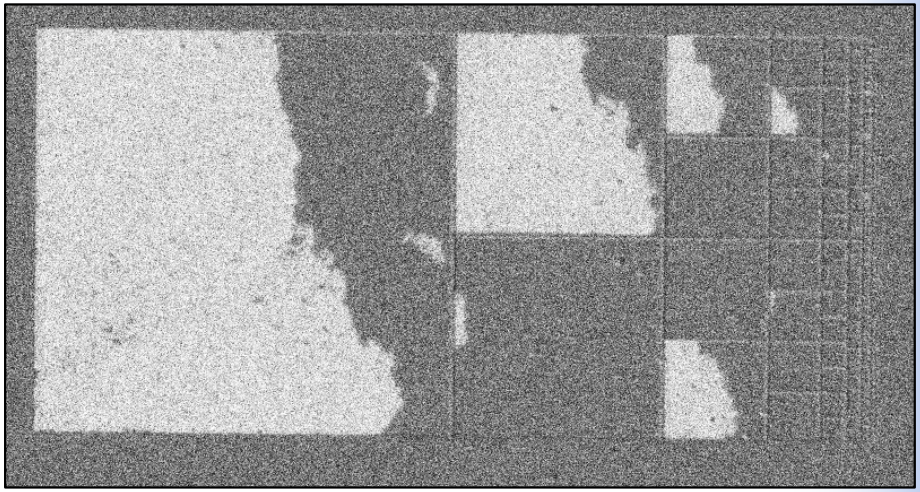

H=36.38 kA/m

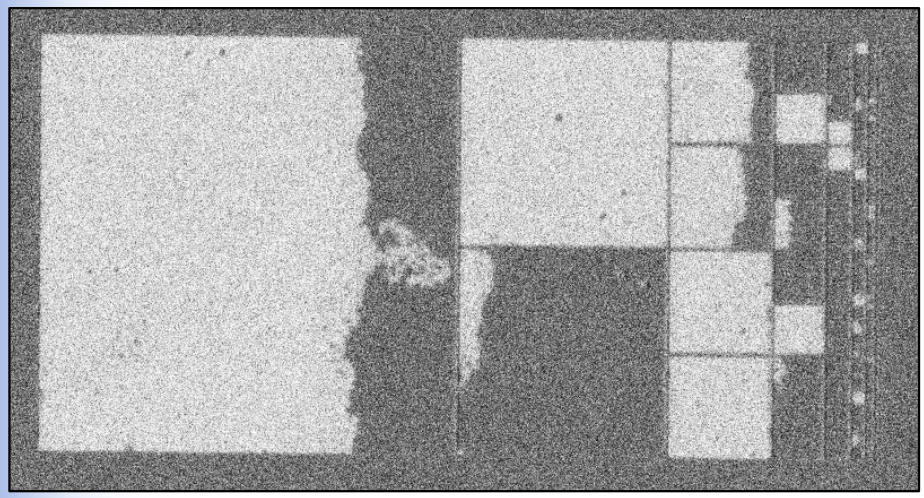

H=37.22 kA/m

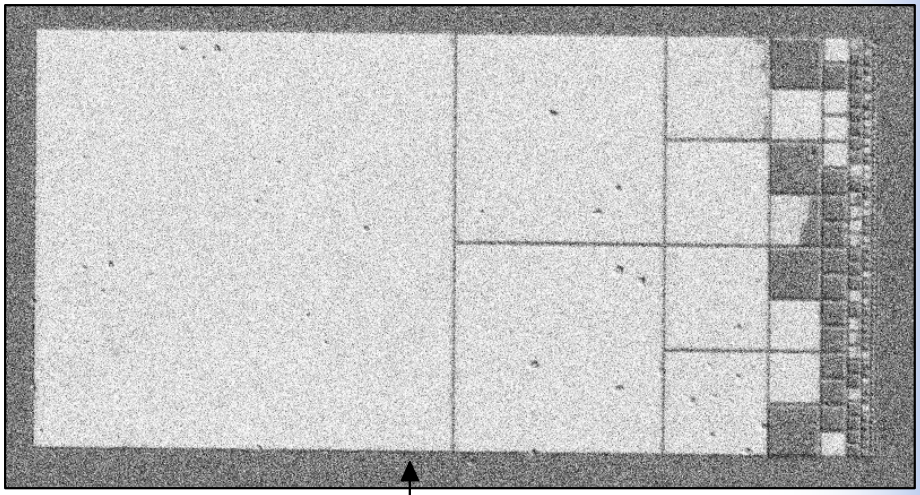

H=37.89 kA/m

256 x 256 µm²

The probability of activating the nucleation center is roughly proportional to element area.

If nucleation centers areal density is low the large elements may reverse while the small ones do not.

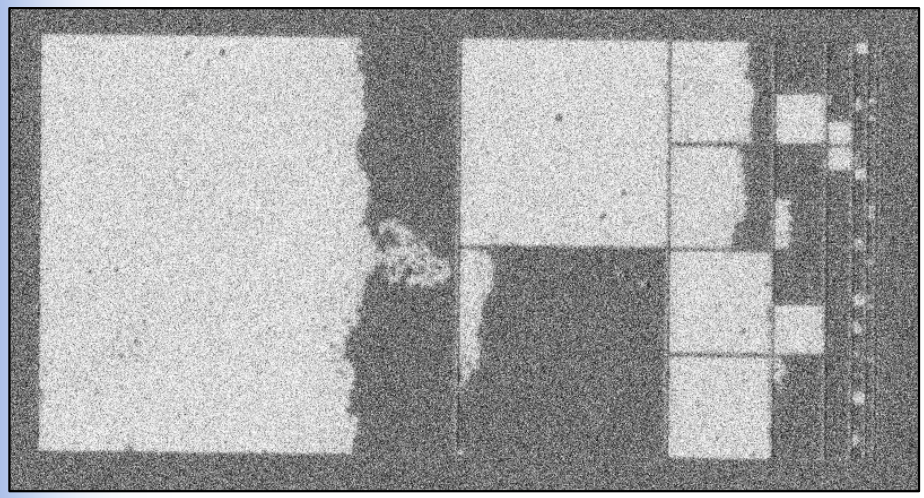

H=37.22 kA/m

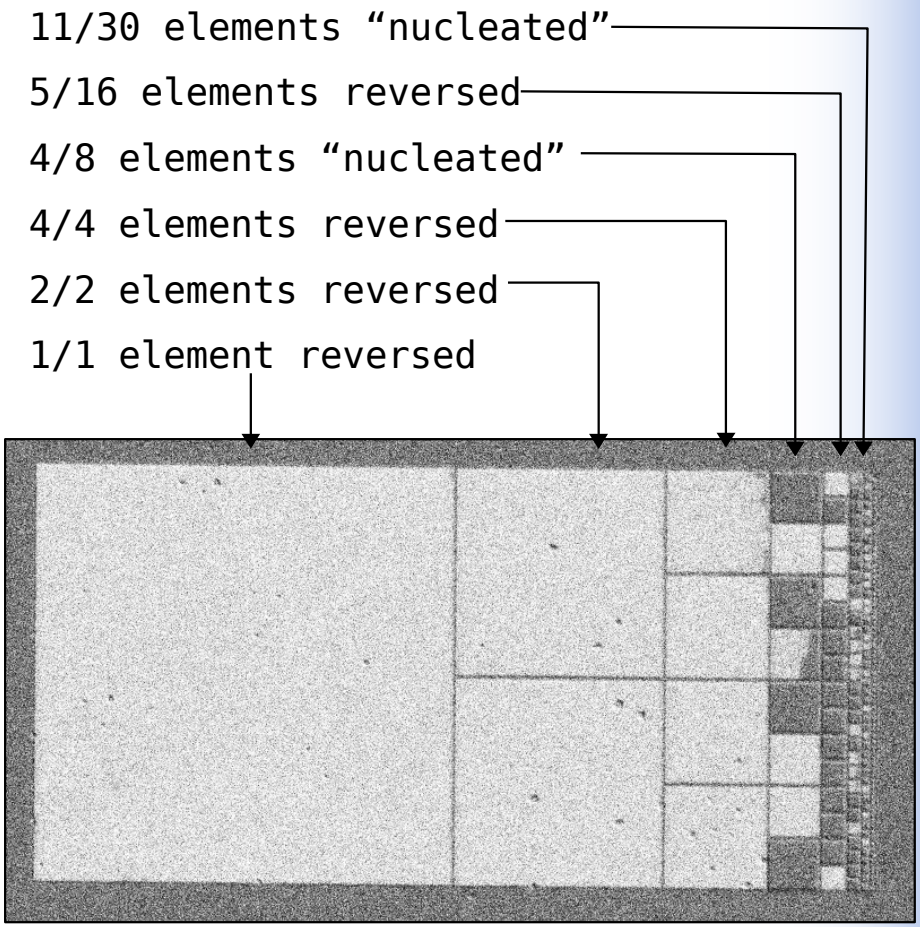


H=37.89 kA/m

# Ion bombardment

- Sample holder moves along the longer edges of the stripes and ion fluence gradient is created along the stripes
- $He^+$ ion fluences are up to $10^{15}$ ion/cm$^2$
- The fluence changes linearly from approx. 0 to $10^{15}$ ion/cm$^2$ over the length of the stripes (990µm)
- The $10^{15}$ ion/cm$^2$ fluence corresponds to approx. **one $He^+$ ion for seven Co atoms**

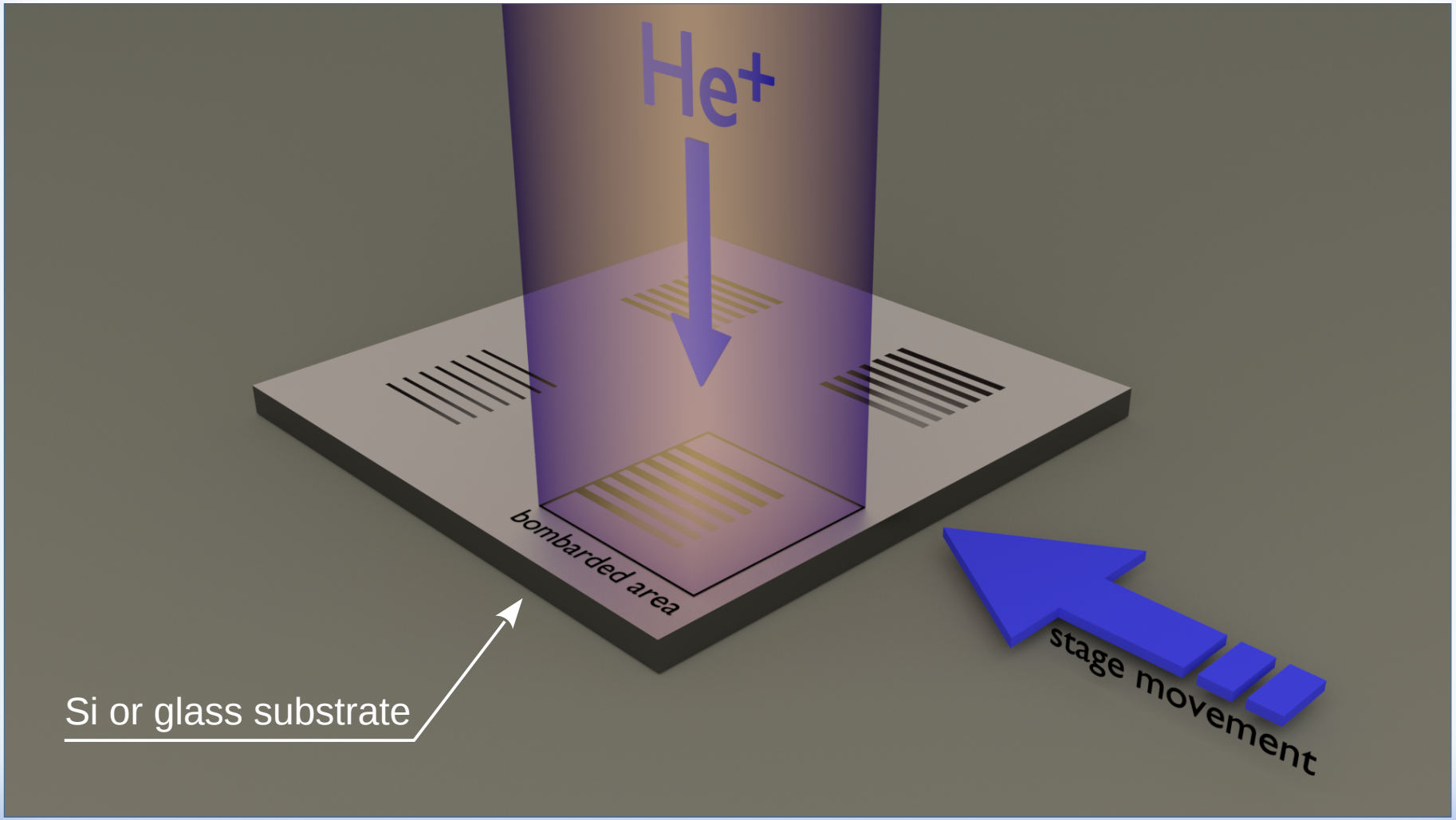




M. Urbaniak, F. Stobiecki, A. Gaul, A. Ehresmann, J. Phys. D: Appl. Phys. **48**, 335003 (2015)

# Ion bombardment

- Sample holder moves along the longer edges of the stripes and **ion fluence gradient is created along the stripes**
- $He^+$ ion fluences are up to $10^{15}$ ion/cm$^2$
- The fluence changes linearly from approx. 0 to $10^{15}$ ion/cm$^2$ over the length of the stripes (990µm)
- The $10^{15}$ ion/cm$^2$ fluence corresponds to approx. one $He^+$ ion for seven Co atoms

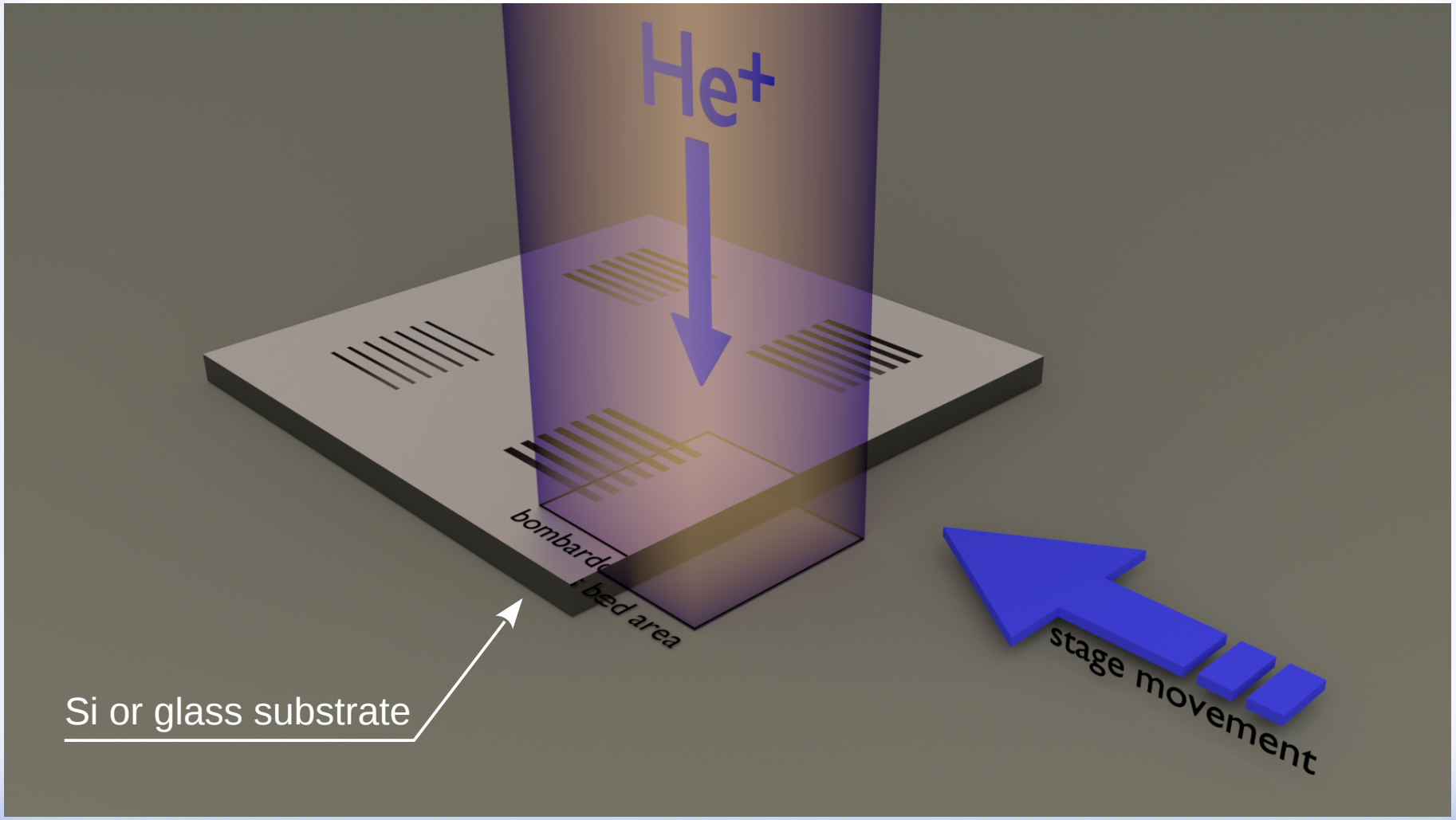




M. Urbaniak, F. Stobiecki, A. Gaul, A. Ehresmann, J. Phys. D: Appl. Phys. **48**, 335003 (2015)

The influence of fluence on coercive field

Si(100)/Ti(4nm)/Au(60nm)/
**[Co(0.8nm)/Au(1nm)]$_2$**

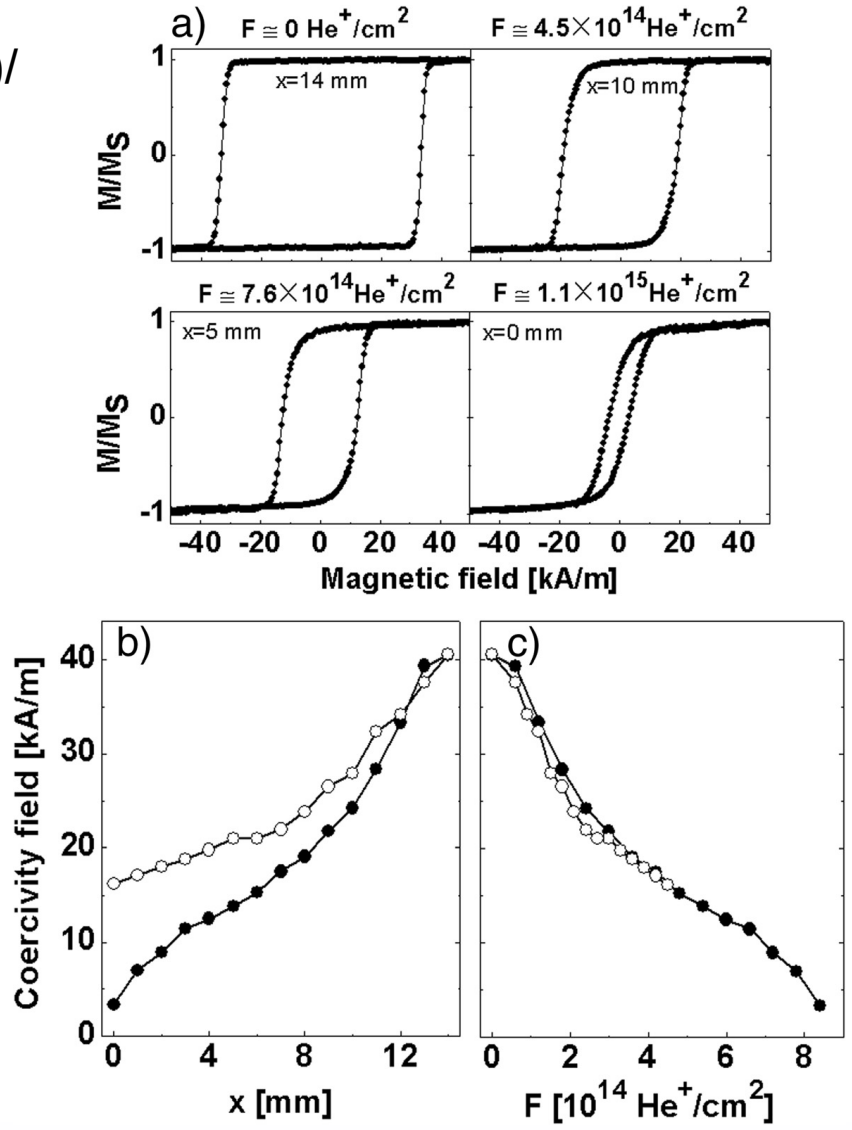


10 keV $He^+$



Matczak *et al.* Nanoscale Research Letters 9, 395 (2014)

# Ion bombardment

- Sample holder moves along the longer edges of the stripes and **ion fluence gradient is created along the stripes**
- $He^+$ ion fluences are up to $10^{15}$ ion/$cm^2$
- The fluence changes linearly from approx. 0 to $10^{15}$ ion/$cm^2$ over the length of the stripes (990µm)
- The $10^{15}$ ion/$cm^2$ fluence corresponds to approx. one $He^+$ ion for seven Co atoms

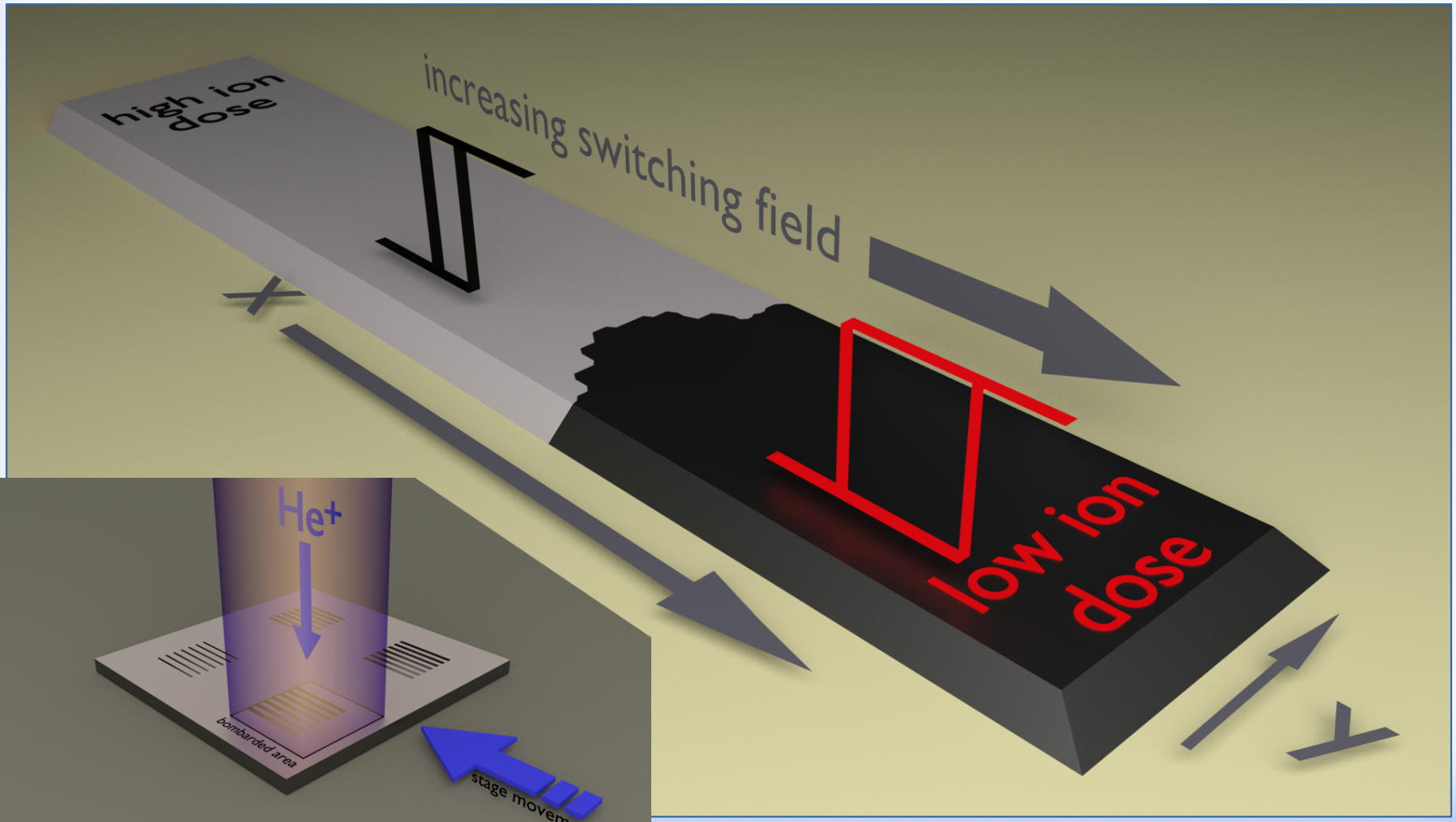

- patterning (EBL) into the stripes increases the coercivity
- possible mechanism: lower number of nucleation centers in small area samples and/or pinning centers introduced during patterning

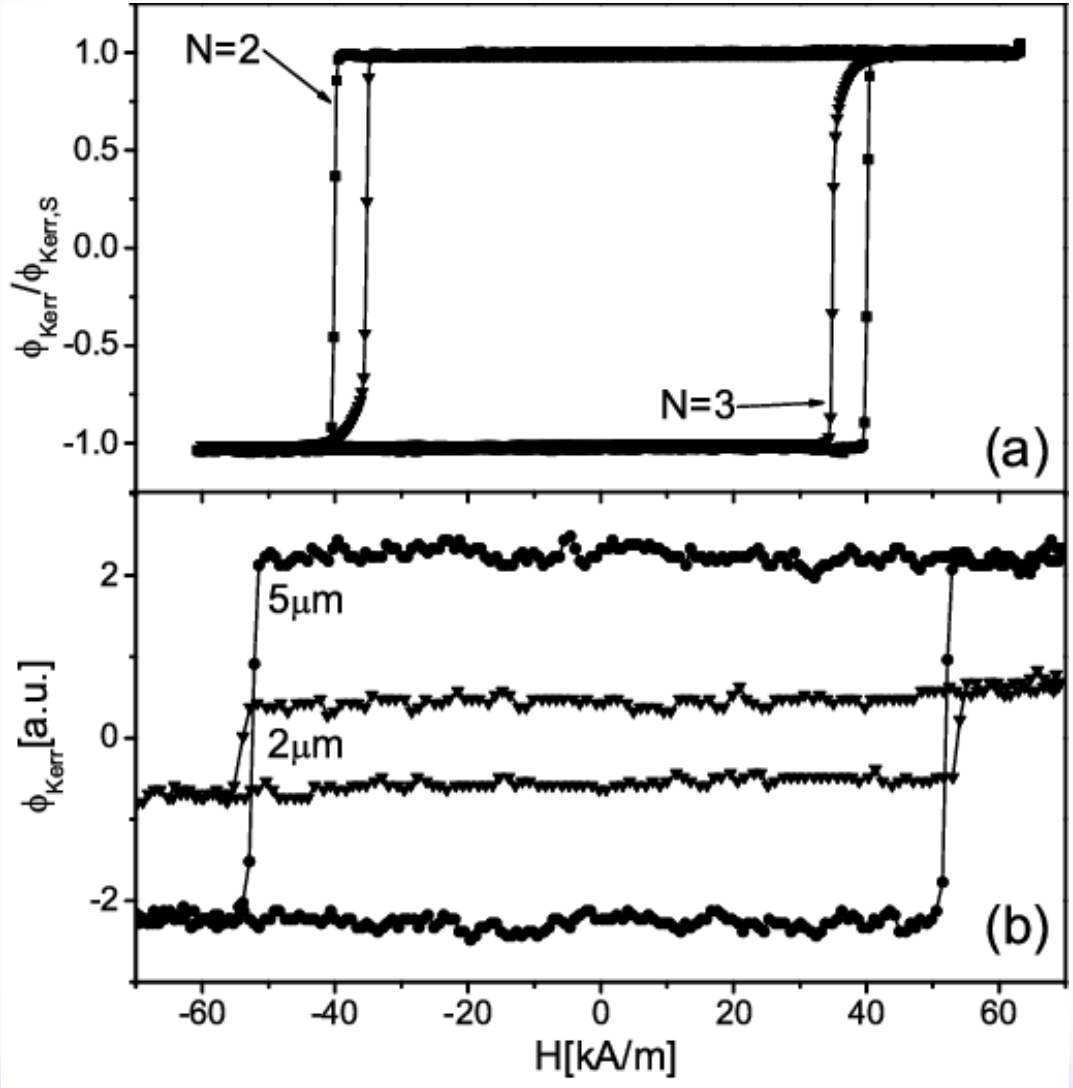


continuous

patterned

(a) Characteristic P-MOKE hysteresis loops of continuous [Co(0.8 nm)/Au(1 nm)]$_N$ MLs.
(b) The analogous loops for the [Co(0.8 nm)/Au(1 nm)]$_2$ layer patterned into 5 and 2 μm wide stripes.

# Nucleation in as-deposited Co PMA stripes

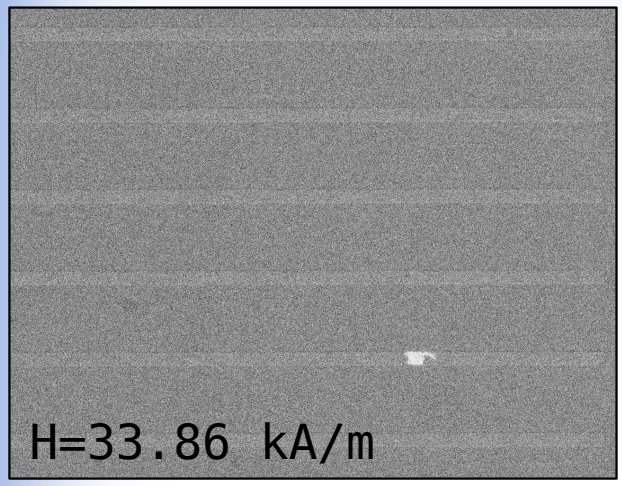


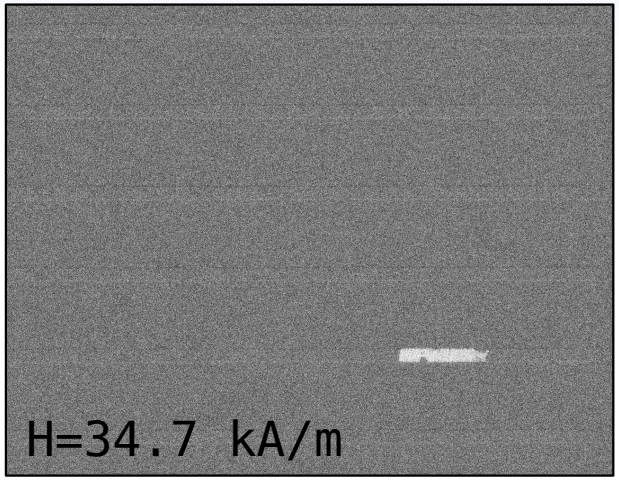


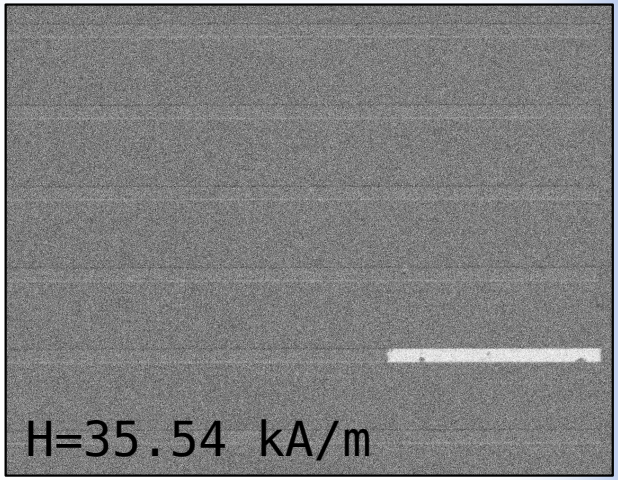


approx. 895×687 μm$^2$

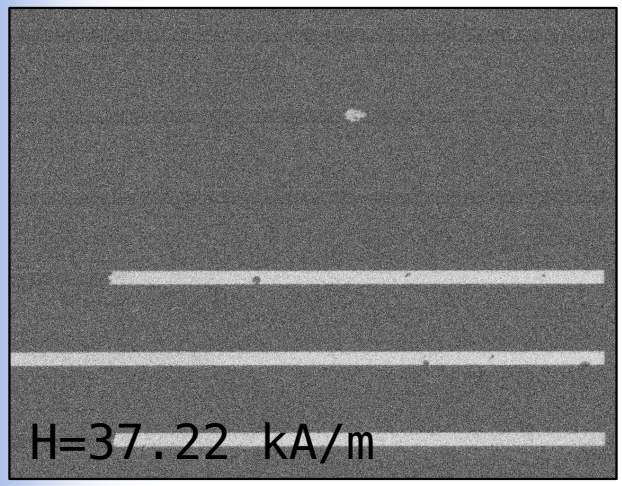


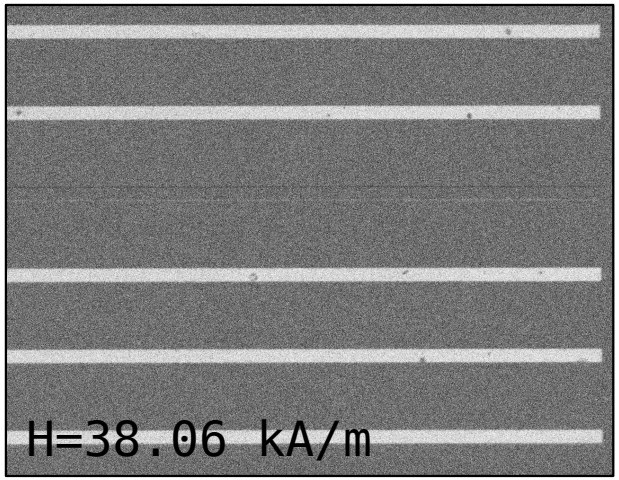


no “active” nucleation center up to 38.06kA/m

$[Co(0.8nm)/Au(1nm)]_3$

- no visible preference for nucleation of domains in any specific area
- a possible preference for the direction of domain propagation may be a result of thickness gradient which is possible in thin films deposition
- note the strong coupling between Co sublayers – single gray level of domain

# Magnetization reversal in bombarded $[Co(0.8nm)/Au(1nm)]_3$ stripes

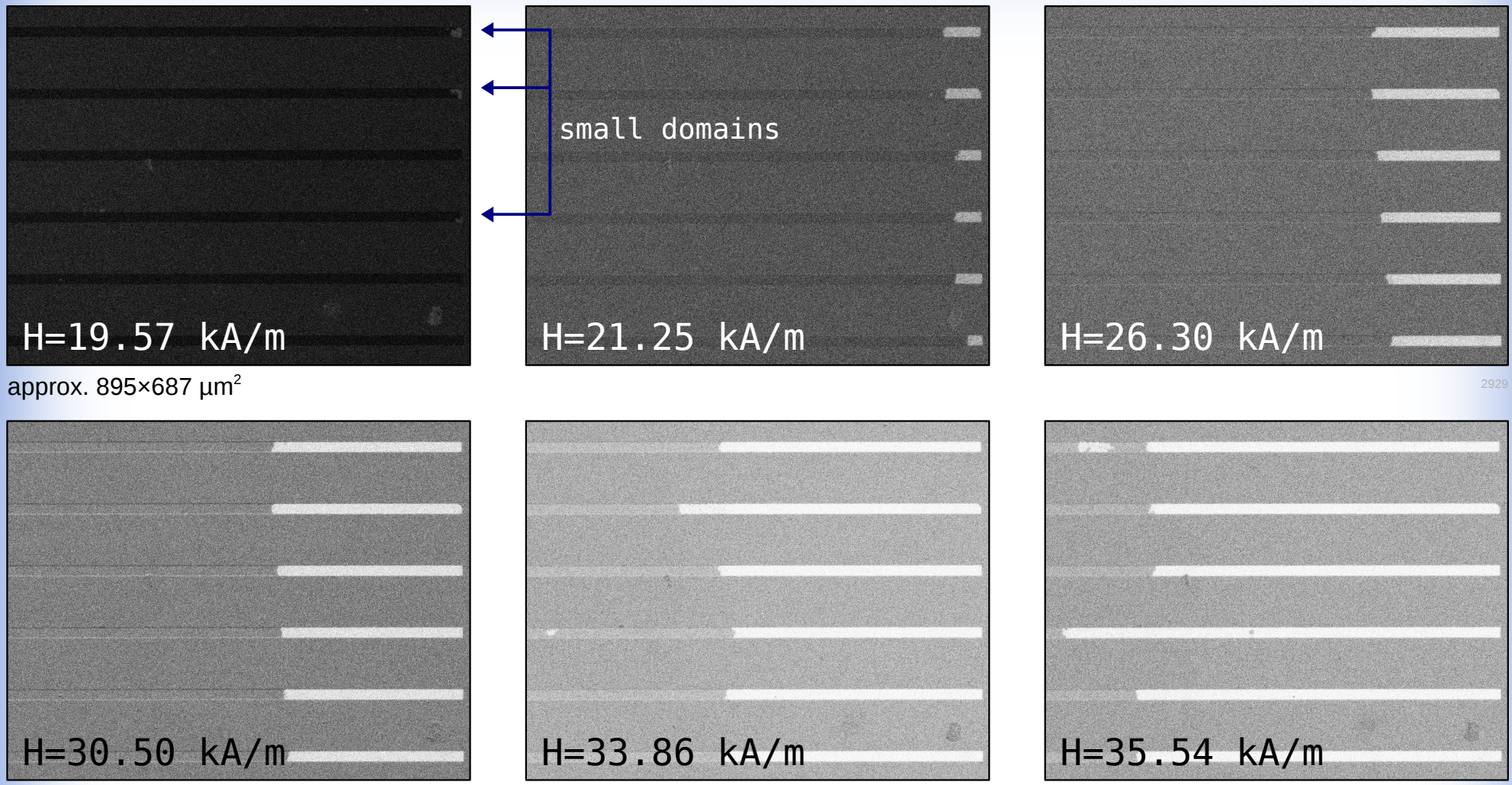


approx. 895×687 μm²

2929

- reversed domains expand from right to left
- note much wider field range (approx. 16 kA/m), as compared to the stripes that were not bombarded (approx. 4 kA/m, previous slide), in which the stripes are not in “single domain” state

M. Urbaniak, F. Stobiecki, A. Gaul, A. Ehresmann, J. Phys. D: Appl. Phys. **48**, 335003 (2015)

# Magnetization reversal in bombarded $[Co(0.8nm)/Au(1nm)]_3$ stripes

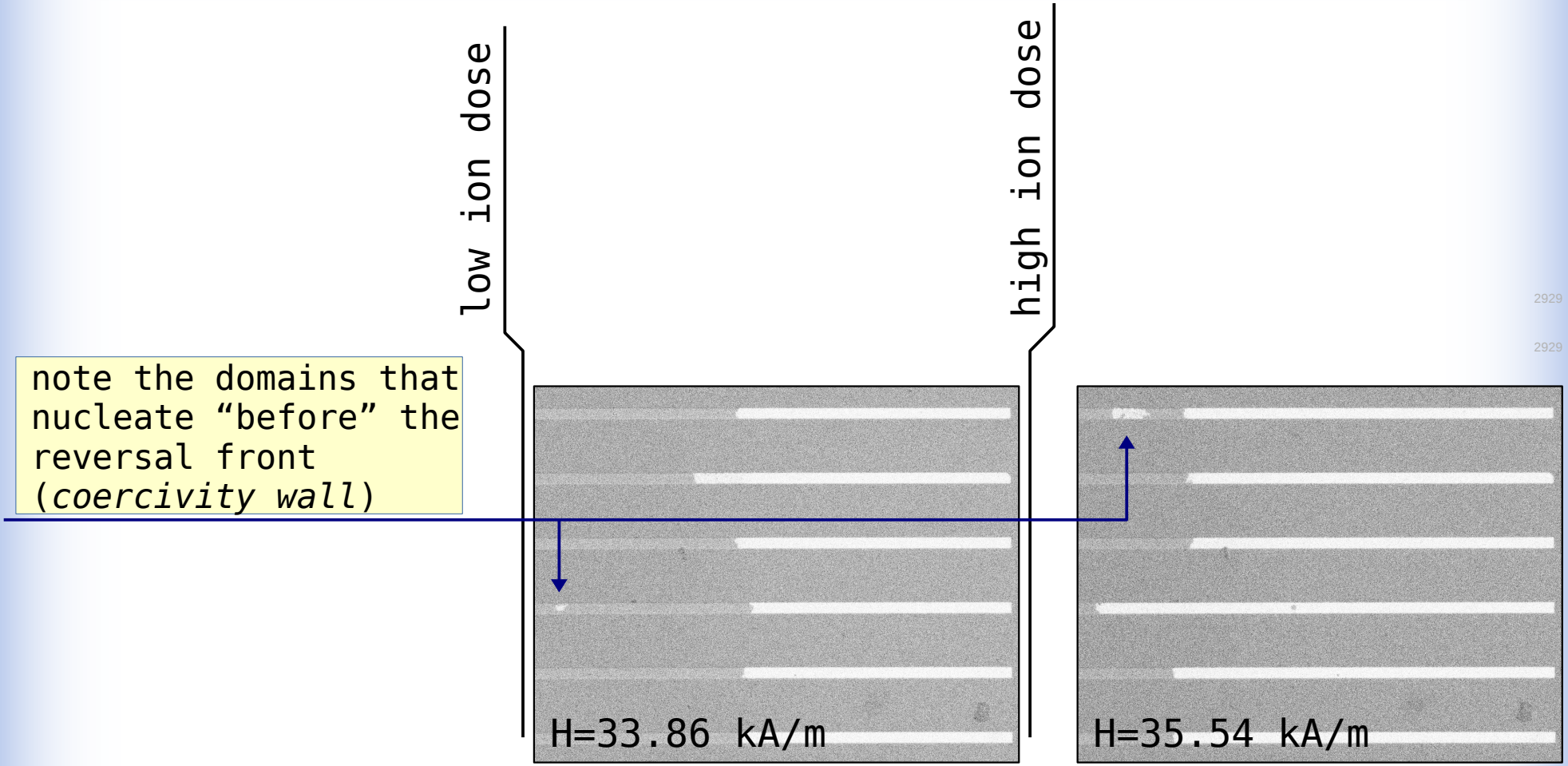


- reversed domains expand from right to left (high dose -> low dose)
- note much wider field range (approx. 16 kA/m), as compared to the stripes that were not bombarded (approx. 4 kA/m, previous slide), in which the stripes are not in “single domain” state

# Magnetization reversal in bombarded $[Co(0.8nm)/Au(1nm)]_3$ stripes

N=2
w=20µm

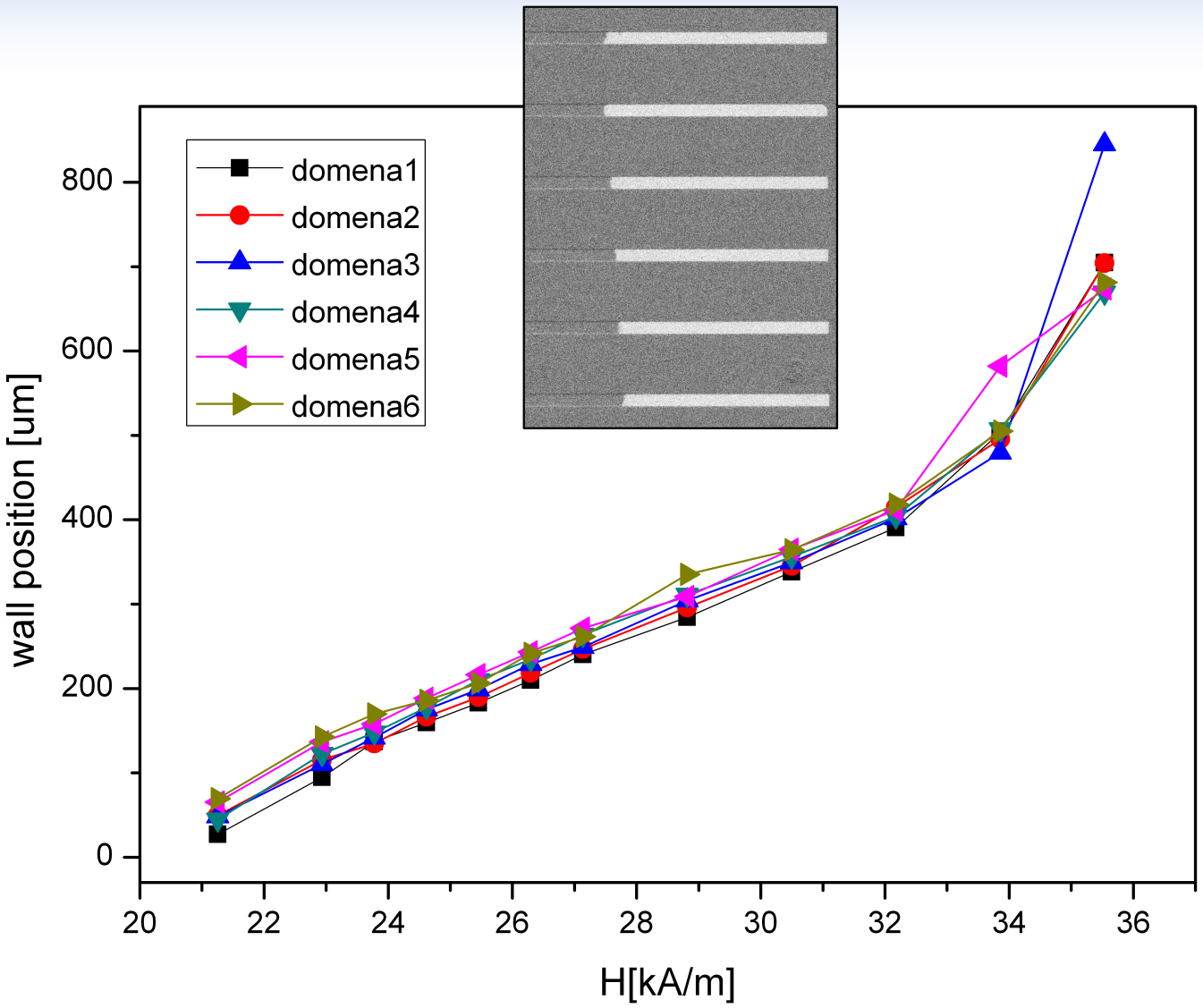


- in all stripes the domain wall position is approximately linear function of the magnetic field pulse strength $H_p$ (for $H_p << H_C$)
- global $H_C$ of the extended reference sample is approx. 35 kA/m and $H_s$ is over 40 kA/m.

# Magnetization reversal in bombarded $[Co(0.8nm)/Au(1nm)]_2$ stripes

N=3
w=20µm

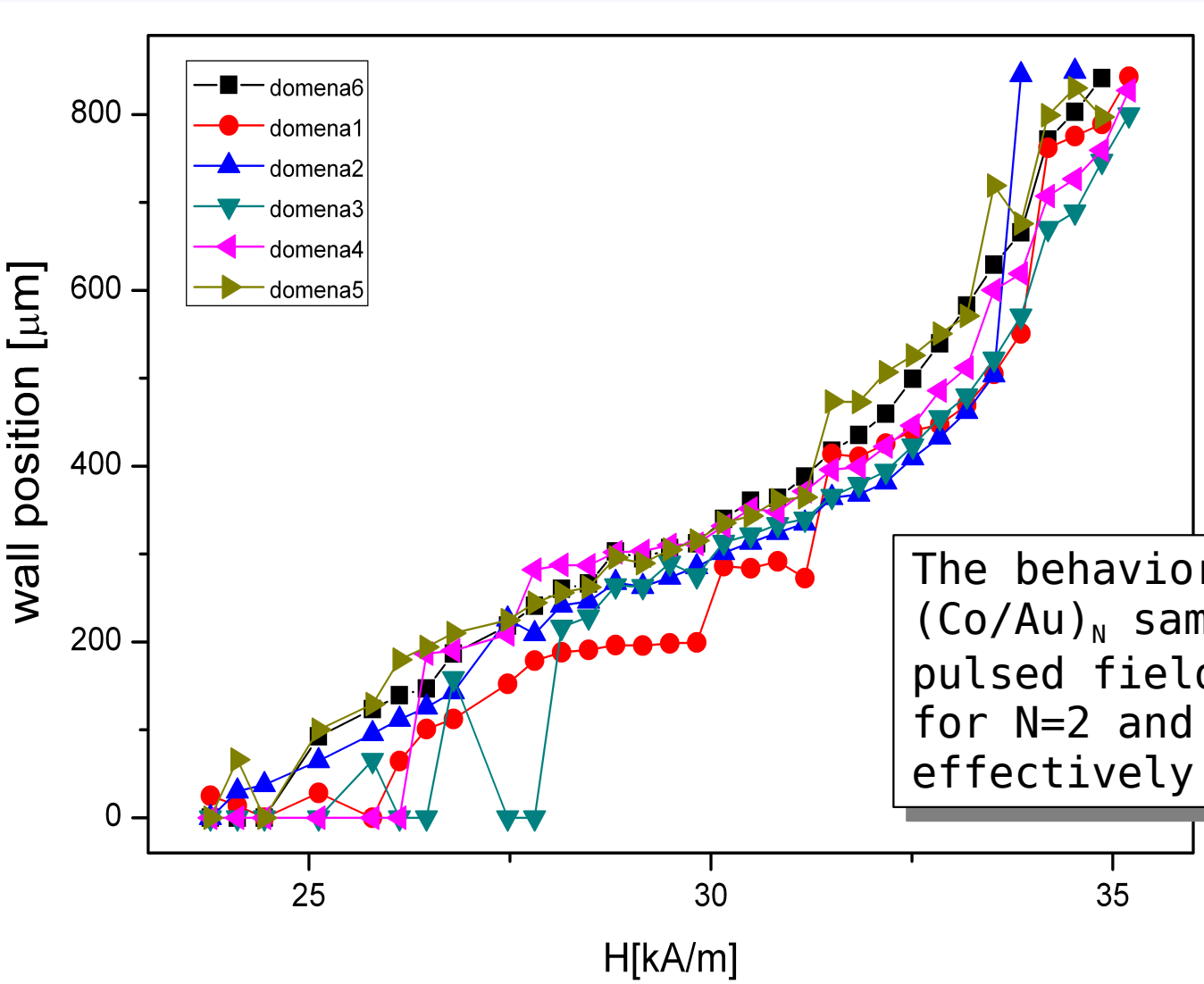


The behavior of the $(Co/Au)_N$ samples in pulsed fields for N=2 and N=3 is effectively the same.

- in all stripes the domain wall position is approximately linear function of the magnetic field pulse strength $H_p$ (for $H_p << H_C$)
- global $H_C$ and $H_s$ of the extended reference sample are approx. 40 kA/m (square loop)

# Magnetization reversal in bombarded $[Co(0.8nm)/Au(1nm)]_2$ stripes

N=3
w=2μm

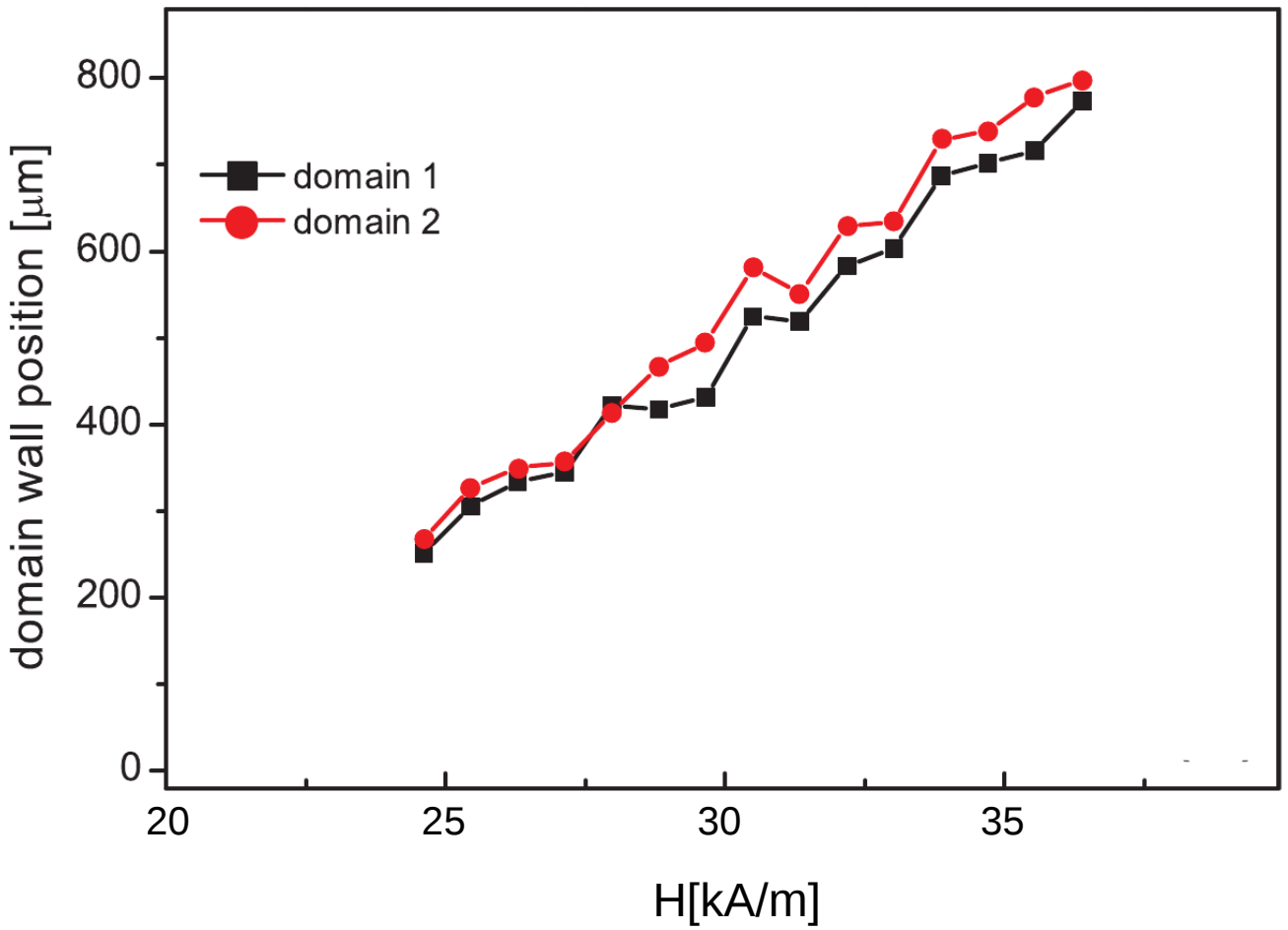


M. Urbaniak, F. Stobiecki, A. Gaul, A. Ehresmann, J. Phys. D: Appl. Phys. **48**, 335003 (2015)

- the behavior of stripes with 2μm is similar (DW position was determined using other procedure than for wider stripes)
- for 1μm the behavior seems to be the same but limited resolution of Kerr microscope did not allow us to quantify this

# Magnetization reversal in bombarded stripes – phenomenological model

- assume that $H_c$ is a measure of $H_n$
- we know the dependence of $H_c$ on ion fluence and the fluence on position along the stripe

$$H_n(x) = H_0 \exp(-x/0.13\,mm)$$

- field dependence of the **barrier height** to nucleation is given by*:

$$\Delta E_n(x) = E_n\left(1 - \frac{H}{H_n(x)}\right)^{1.5}$$

- the magnetization reversal can be activated thermally and its rate, r, or frequency may be described by an **Arrhenius type law**

$$r(x,T) = r_0 \exp\left(\frac{-\Delta E_n(x)}{k_B T}\right)$$

- we divide the stripe, along its length, into 1000 pieces/cells and for each of them calculate reversal rate
- for each cell, using random numbers and the reversal rate, we decide whether it becomes a nucleation center
- each domain is allowed to grow by 20 cells in both directions during the application of the field

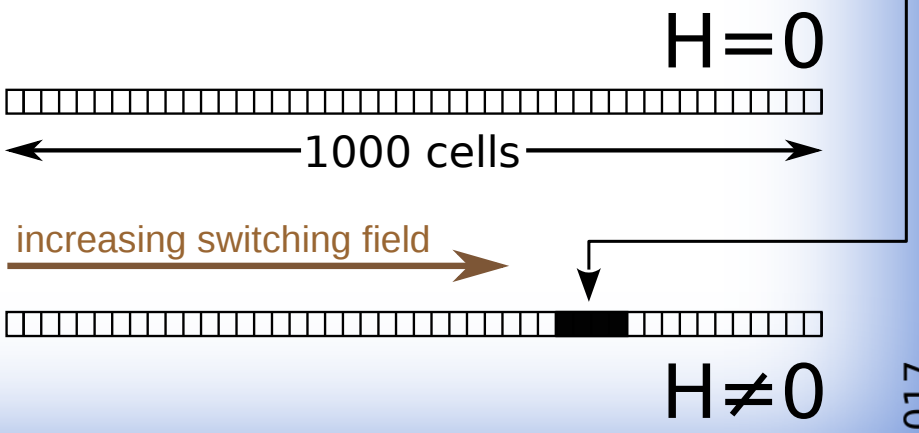


*J. Vogel, J. Moritz, and O. Fruchart, C.R. Phys. 7, 977 (2006)

# Magnetization reversal in bombarded stripes – phenomenological model

- like in the experiment the domains grow with increasing H
- for some values of H domains nucleate to the right of the reversal front
- in some cases the length of the domain is less for higher H, as is observed experimentally

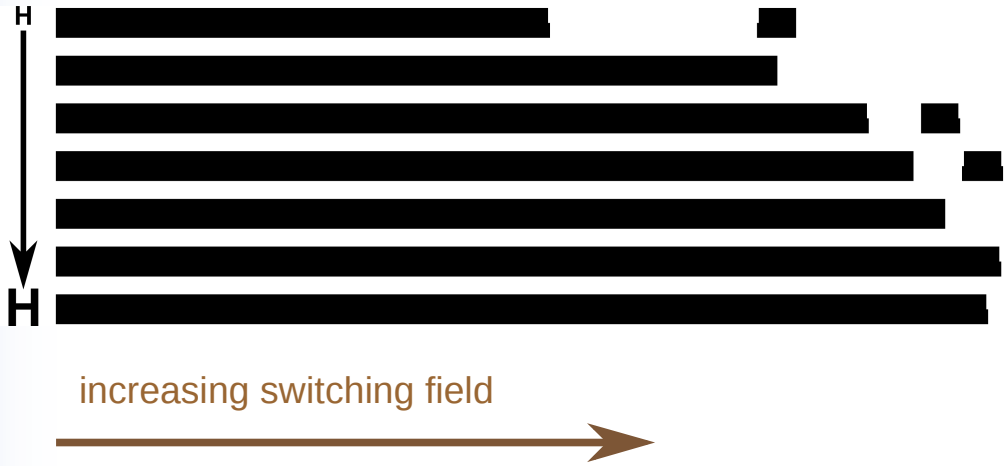


Exemplary simulated magnetic configuration obtained from the phenomenological model. The field pulse strength increases from the top to bottom stripe (H = 0.01, 0.05, 0.10, 0.15, 0.2, 0.25, 0.3 [a.u.]). The parameters used in the model are: $H_0 = 1$, $E_n = 1$, $r_0 = 1$, $k_B = 1$ , and $T = 0.1$.

# Co/Pt multilayers with coupling gradient

- sputtered
- two Co layers with different coercivity which is determined by the thickness of the layers
- coupling changes with position along the platinum wedge

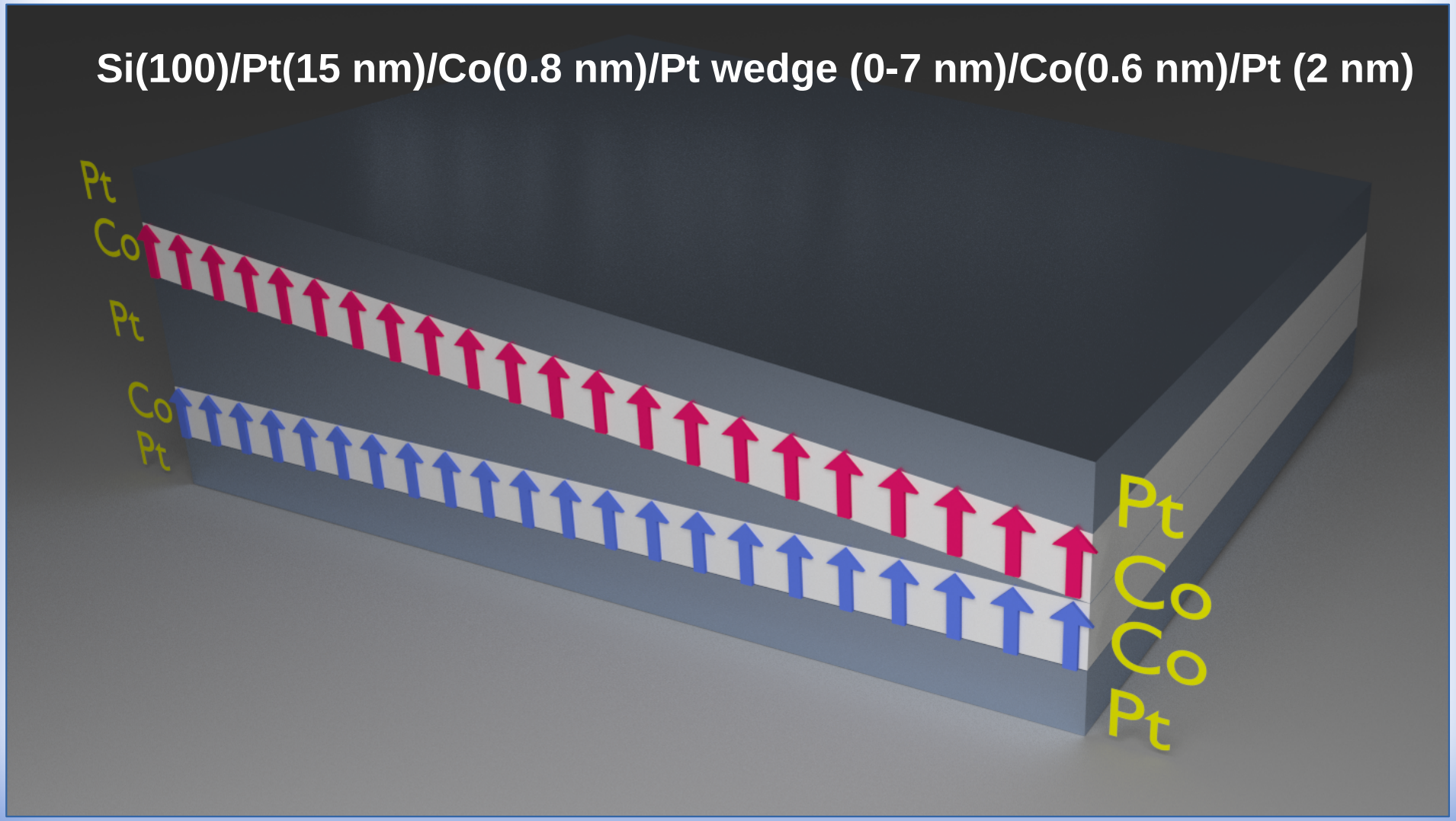


M. Matczak *et al.*, Appl. Phys. Lett. **107**, 012404 (2015)

# Co/Pt multilayers with coupling gradient

How to influence the position of the domain wall?

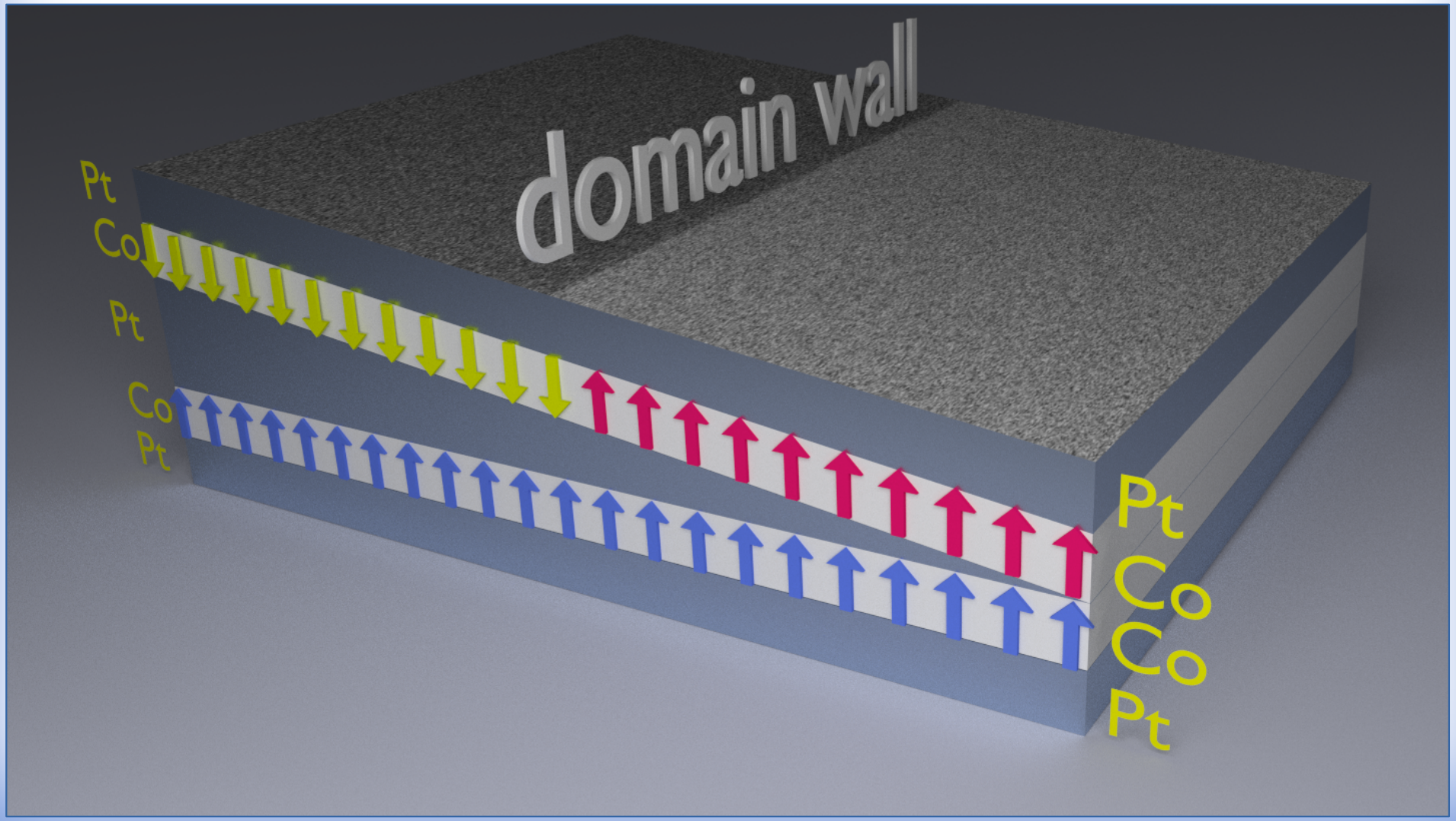


M. Matczak *et al.*, Appl. Phys. Lett. **107**, 012404 (2015)

# Co/Pt multilayers with coupling gradient

- the local hysteresis loop depends on the strength of the coupling between Co layers parted by platinum spacer
- thick Pt spacer – both layers reverse independently

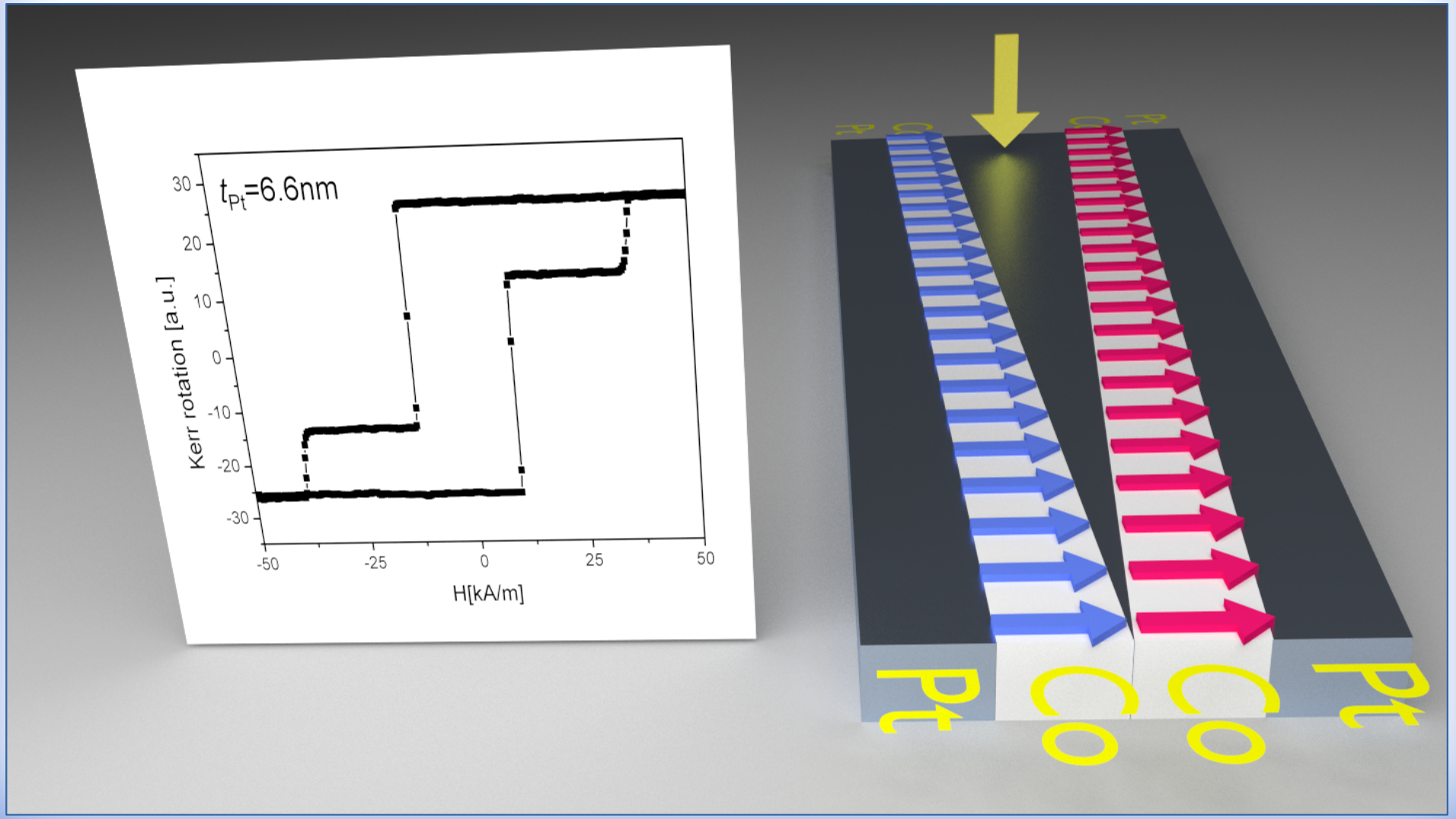

# Co/Pt multilayers with coupling gradient

- the local hysteresis loop depends on the strength of the coupling between Co layers parted by platinum spacer
- intermediate Pt thickness – the switching fields of both Co layers are position dependent

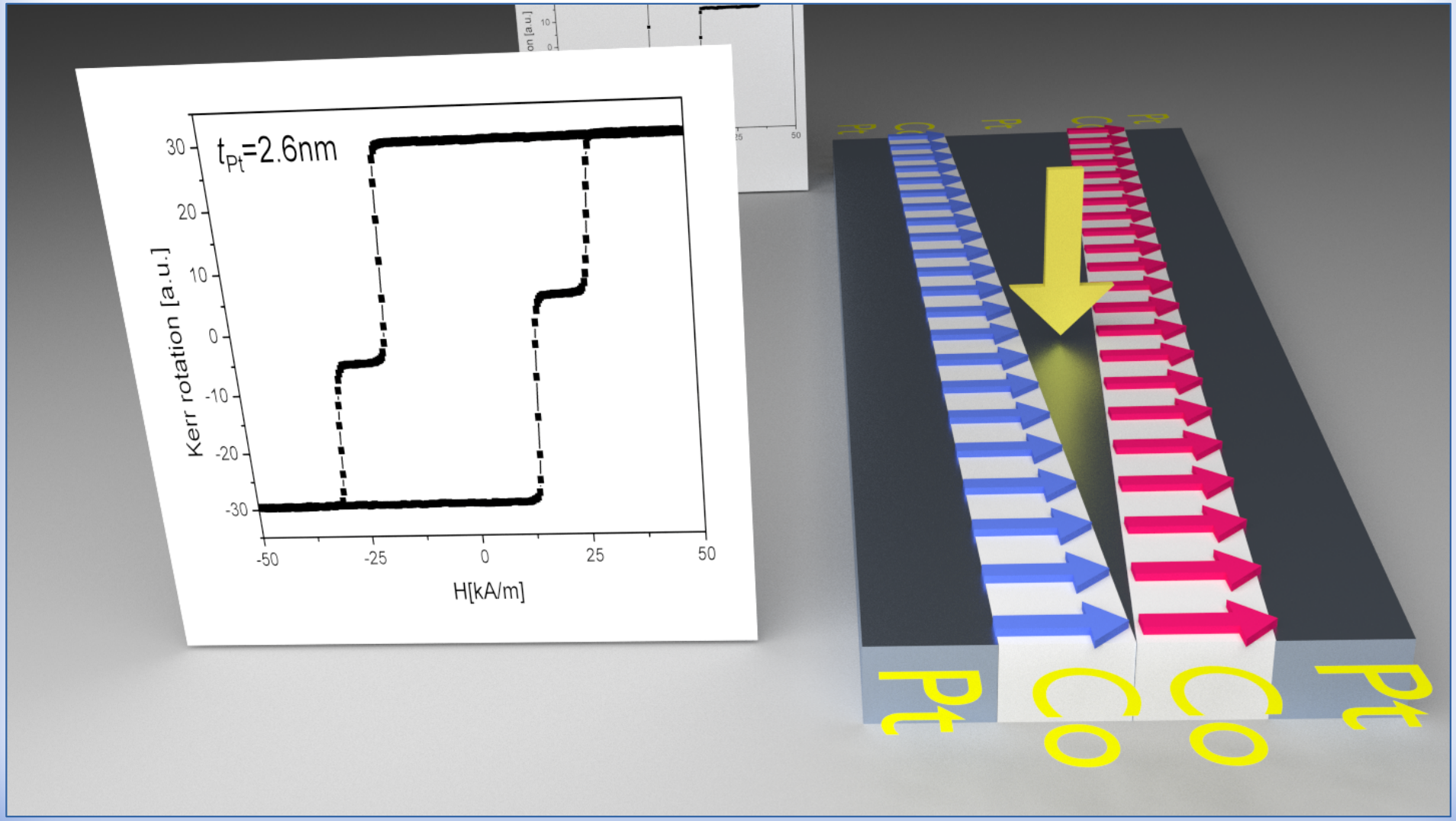

# Co/Pt multilayers with coupling gradient

- the local hysteresis loop depends on the strength of the coupling between Co layers parted by platinum spacer
- thin Pt spacer – cooperative switching of both Co layers

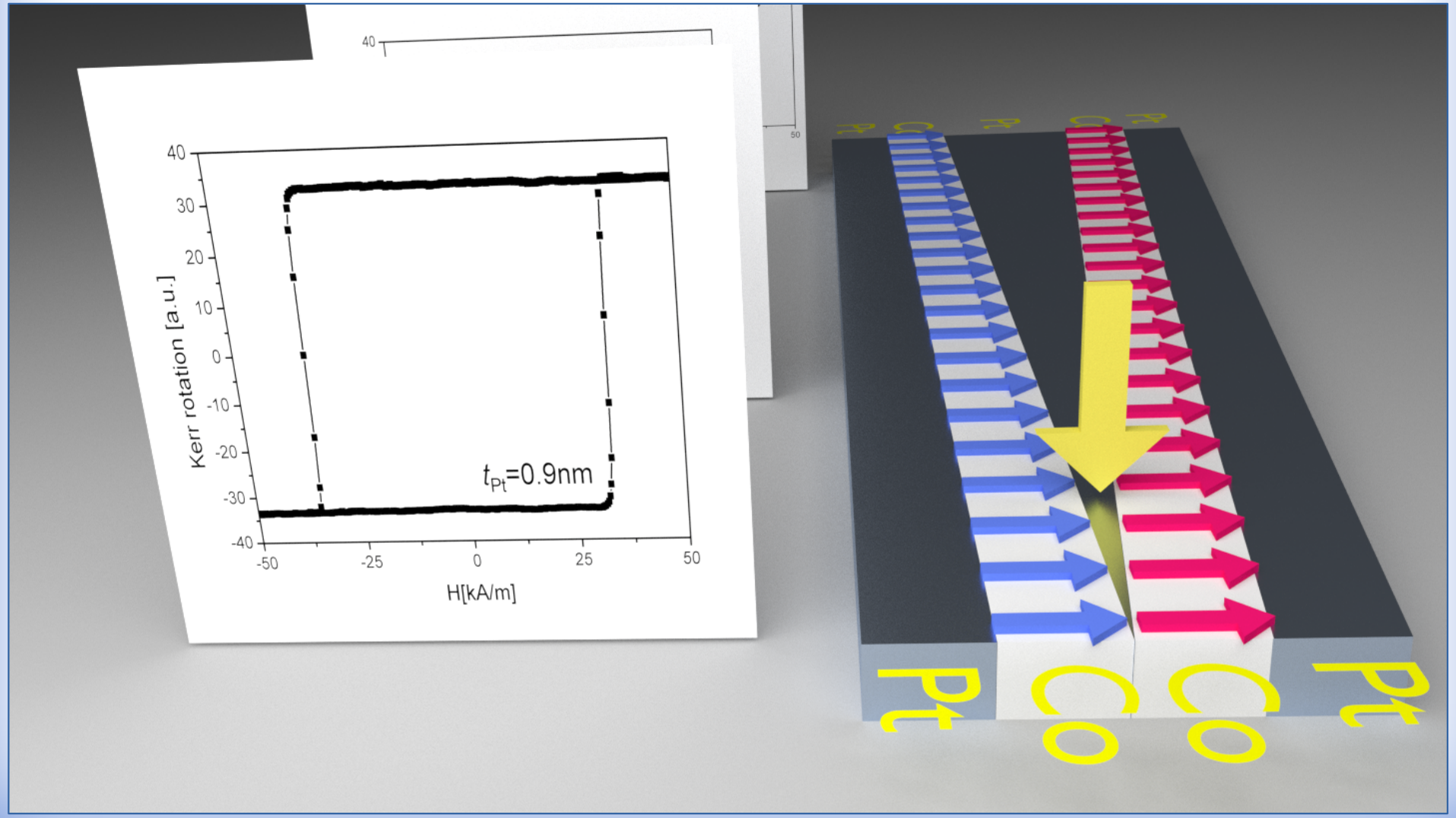

# Co/Pt multilayers with coupling gradient

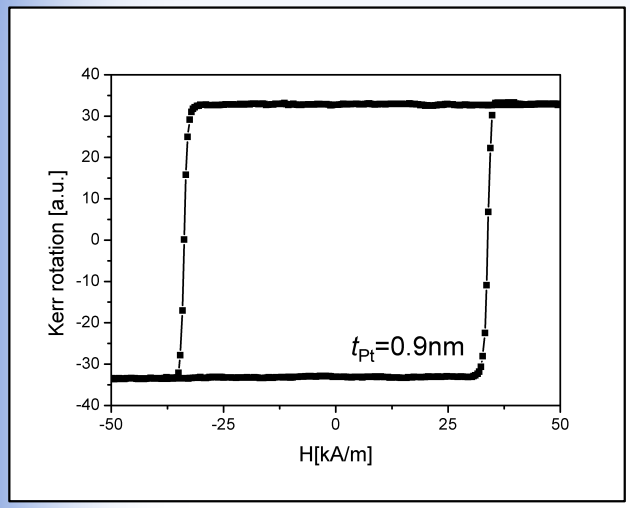


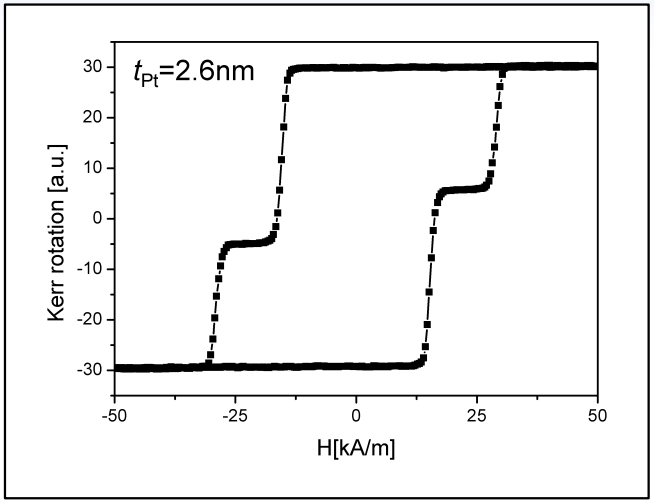


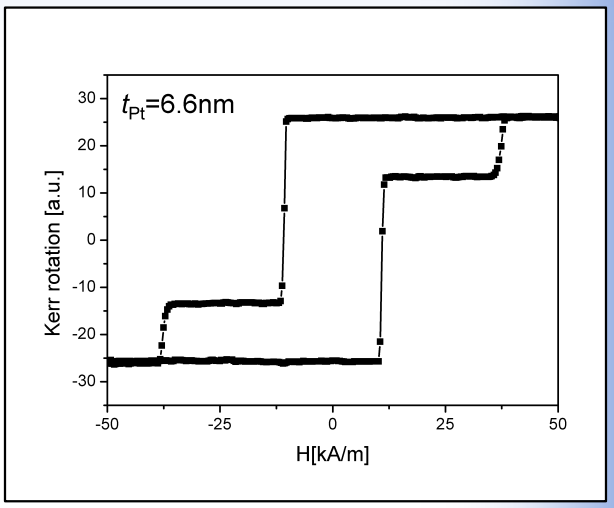


**Si(100)/Pt(15 nm)/Co(0.8 nm)/Pt wedge (0-7 nm)/Co(0.6 nm)/Pt(2 nm), N=2**

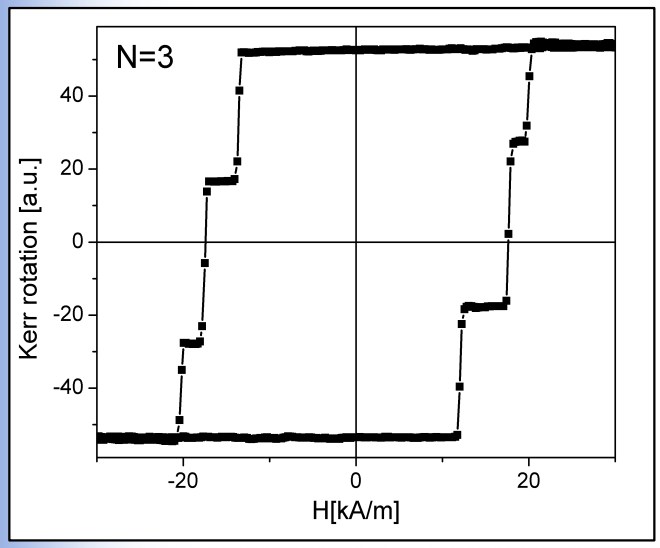


- In multilayers the switching fields of various layers are usually different due to different growth conditions, differing behavior of outer layers etc.
- Simultaneous switching may suggest the interlayer coupling

**Si(100)/Ti(15 nm)/Au(40 nm)/[Au(2nm)/Co(0.5 nm)]$_3$ /Au(2 nm), N=3**



M. Matczak *et al.*, Appl. Phys. Lett. **107**, 012404 (2015)

# Co/Pt multilayers with coupling gradient

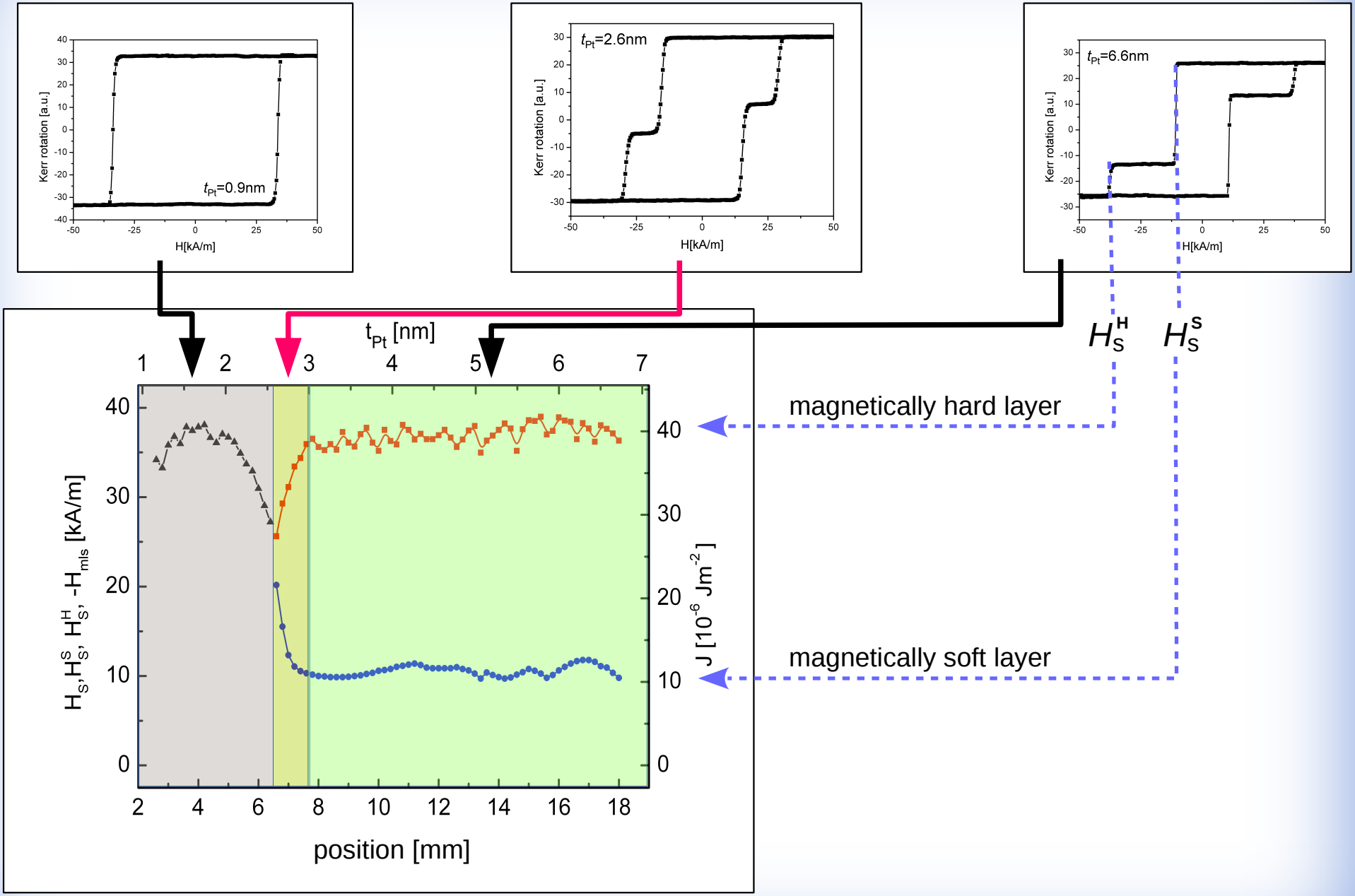


**Si(100)/Pt(15 nm)/Co(0.8 nm)/Pt wedge (0-7 nm)/Co(0.6 nm)/Pt(2 nm), N=2**

M. Matczak *et al.*, Appl. Phys. Lett. **107**, 012404 (2015)

# Co/Pt multilayers with coupling gradient

we investigated mainly the Pt thickness range corresponding to significant gradient of the coupling between Co layers

the shift of the minor hysteresis loop $H_{mls}$ of the magnetically soft layer, if the magnetization of the hard layer is "up", is a measure of the coupling between Co layers

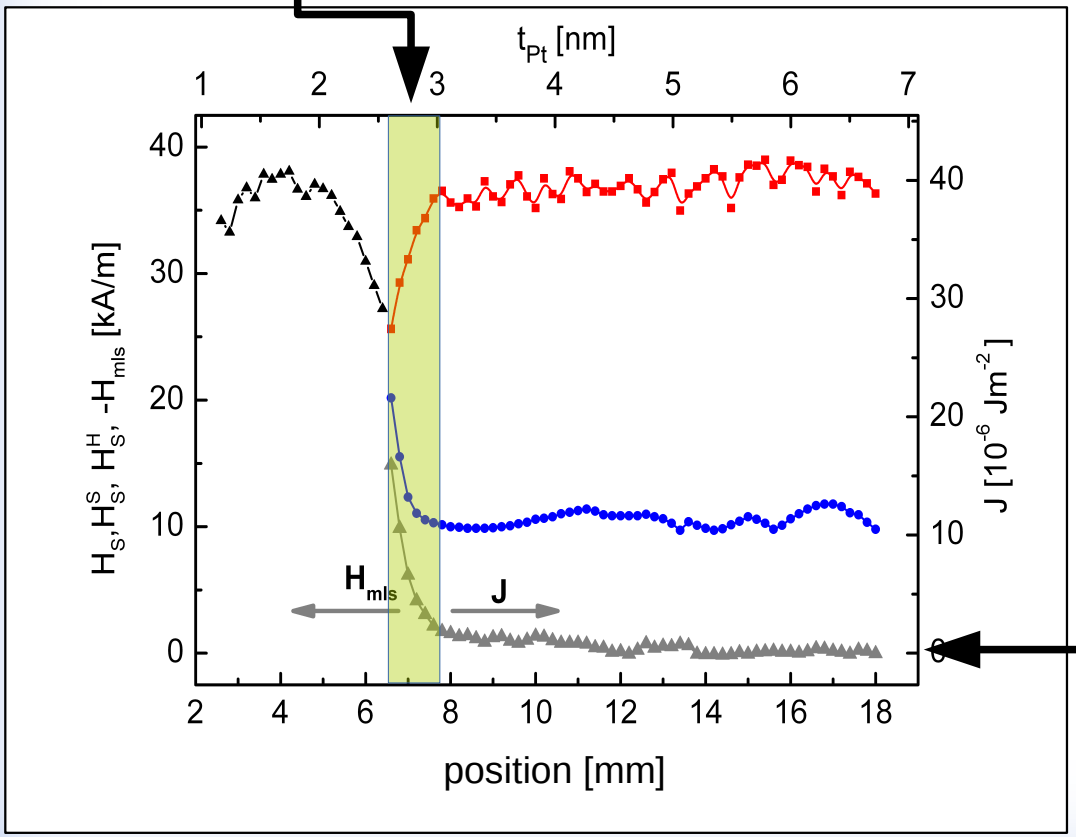


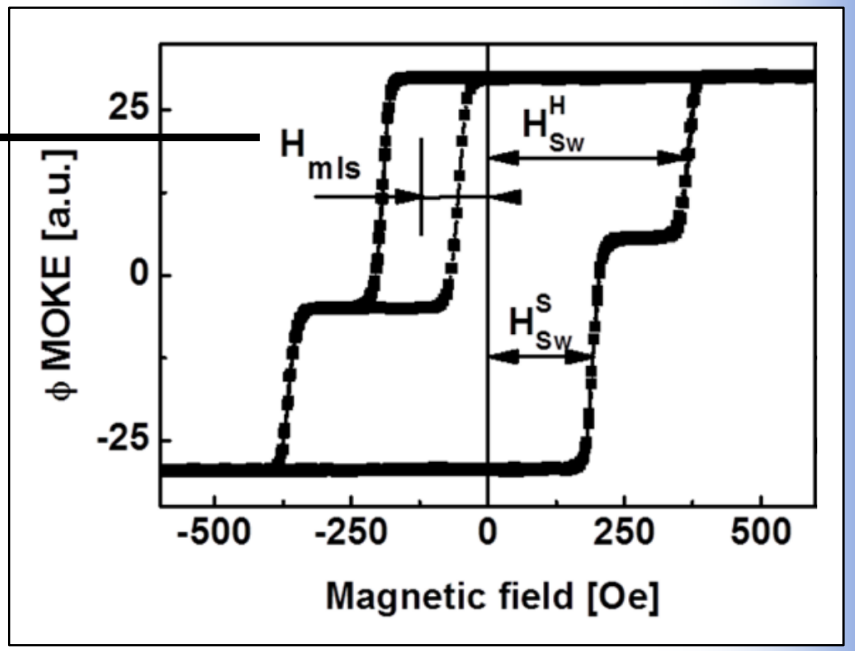


**Si(100)/Pt(15 nm)/Co(0.8 nm)/Pt wedge (0-7 nm)/Co(0.6 nm)/Pt(2 nm), N=2**

M. Matczak *et al.*, Appl. Phys. Lett. **107**, 012404 (2015)

In the thickness range corresponding to a weak interlayer coupling the domain propagates in the “creep” regime

$$v = v_0 \exp\left[-\frac{P}{H^{1/4}}\right]$$

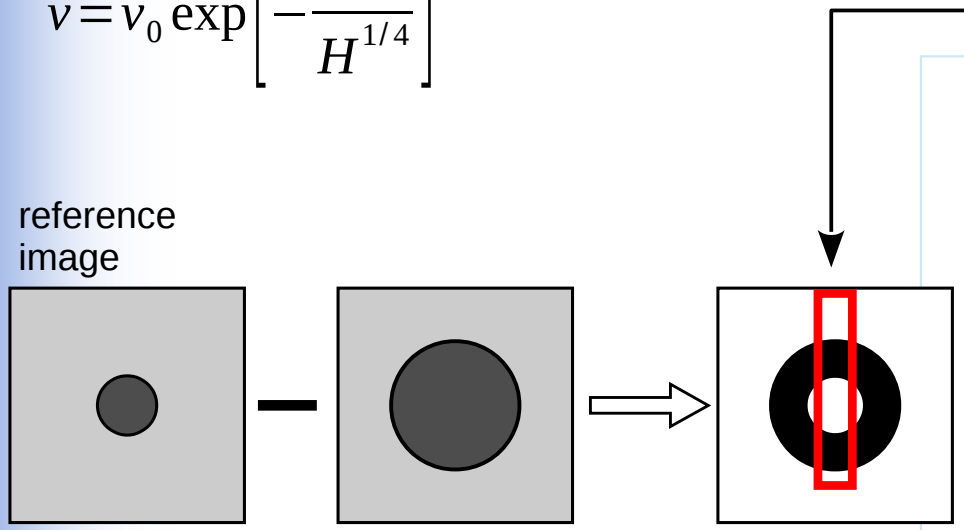


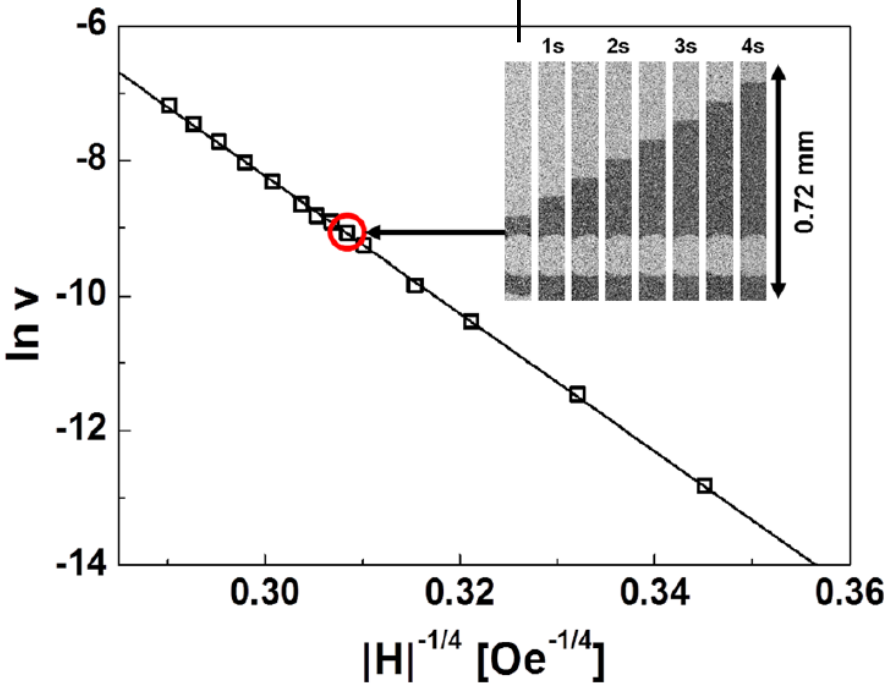


FIG. 3. Natural logarithm of the DW velocity $v$ (expressed in m/s), in the $Co^S$ layer versus $H^{-1/4}$ for a $Co^H$ /Pt-wedge/$Co^S$ layered film determined for a spacer layer thickness $t_{Pt} = 6.6$ nm ($x = 17$ mm), i.e., in the range corresponding to a weak interlayer coupling. The inset shows difference domain images where the upper dark area corresponds to the area reversed by the sum of consecutive field pulses.

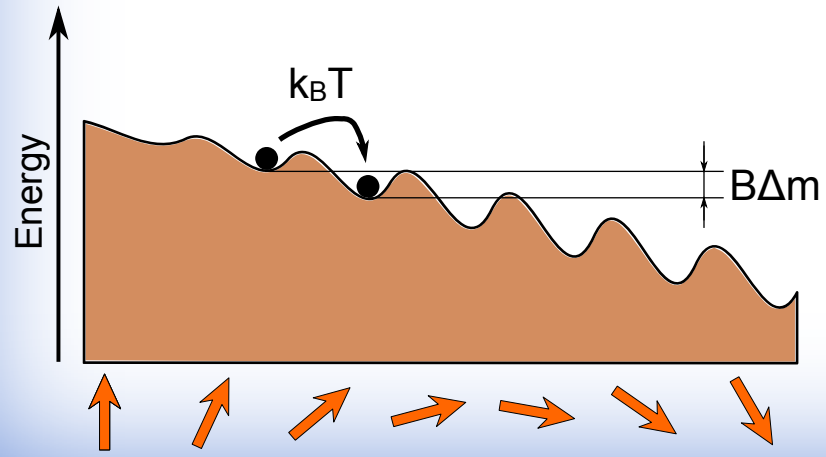


M. Matczak *et al.*, Appl. Phys. Lett. **107**, 012404 (2015)

# Co/Pt multilayers with coupling gradient

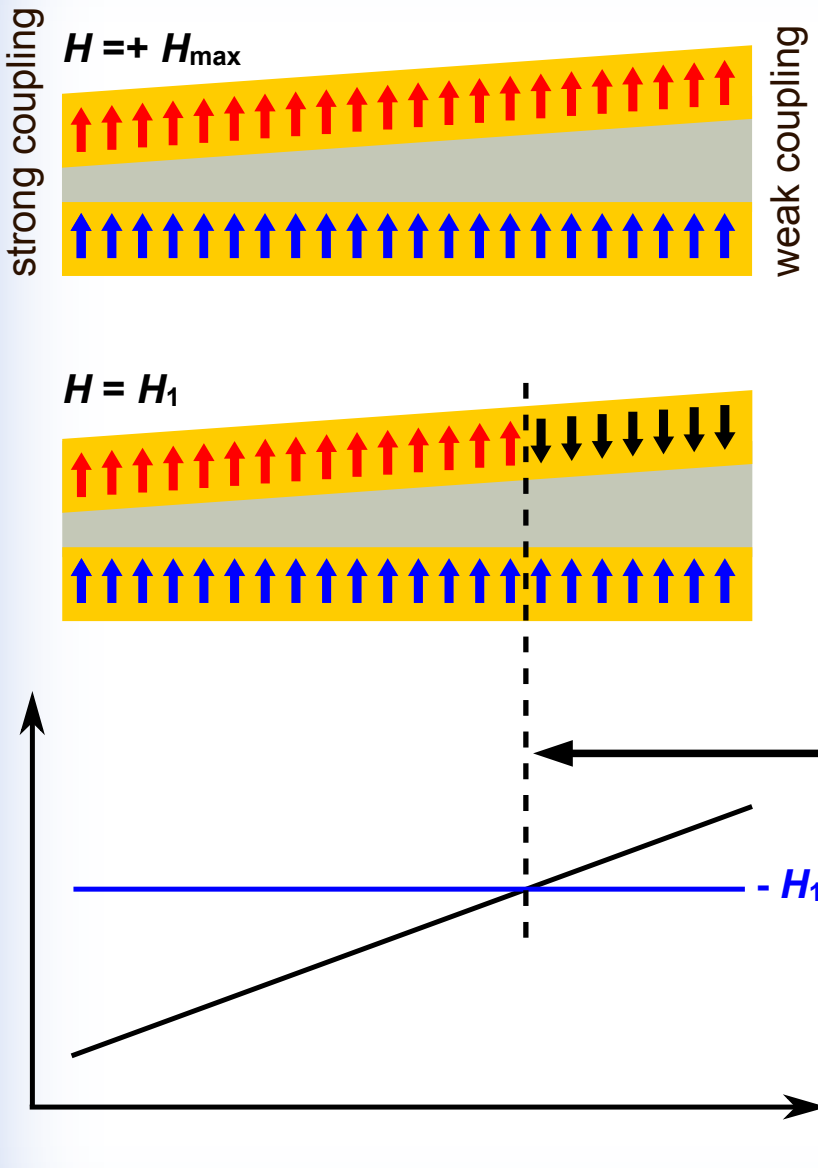


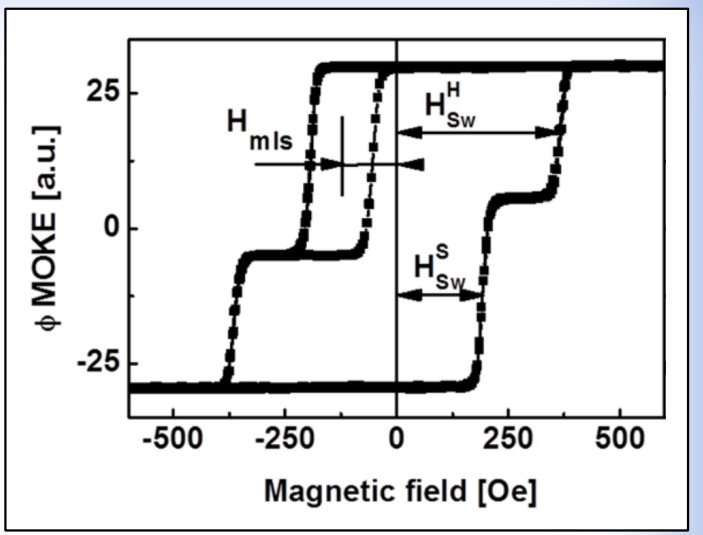


In the external field $H=-H_{mls}(x)$ the effective field acting on the spins positioned at x is zero.

- effective local field acting on the spins of the soft layer is a sum of the external field and the coupling field between Co layers
- the effective field is a function of position (x)

M. Matczak *et al.*, Appl. Phys. Lett. **107**, 012404 (2015)

# Co/Pt multilayers with coupling gradient

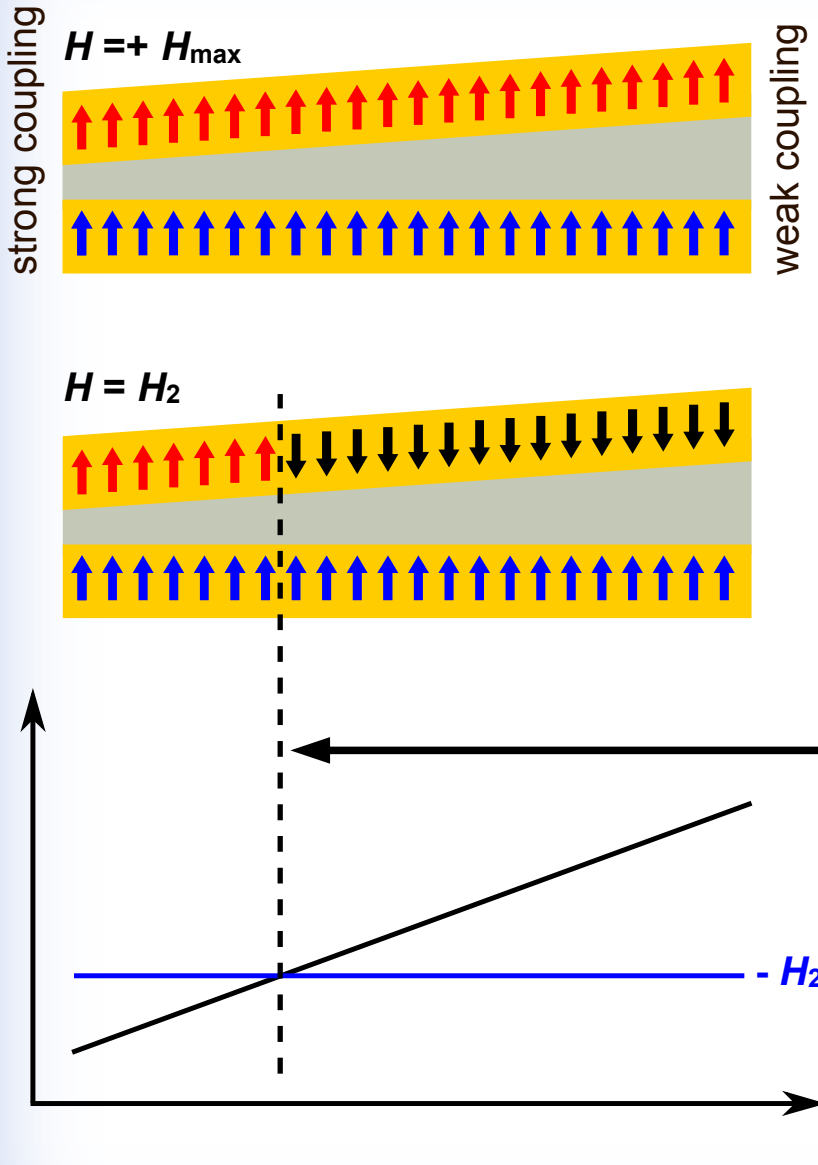


$$v = v_o \exp\left[-\frac{P}{\left(|H - H_{mls}|\right)^{(1/4)}}\right]$$

In the external field $H=-H_{mls}(x)$ the effective field acting on the spins positioned at x is zero.

- effective local field acting on the spins of the soft layer is a sum of the external field and the coupling field between Co layers
- ehe effective field is a function of position (x)

M. Matczak *et al.*, Appl. Phys. Lett. **107**, 012404 (2015)

Domain wall propagation in the presence of the gradient of ferromagnetic coupling

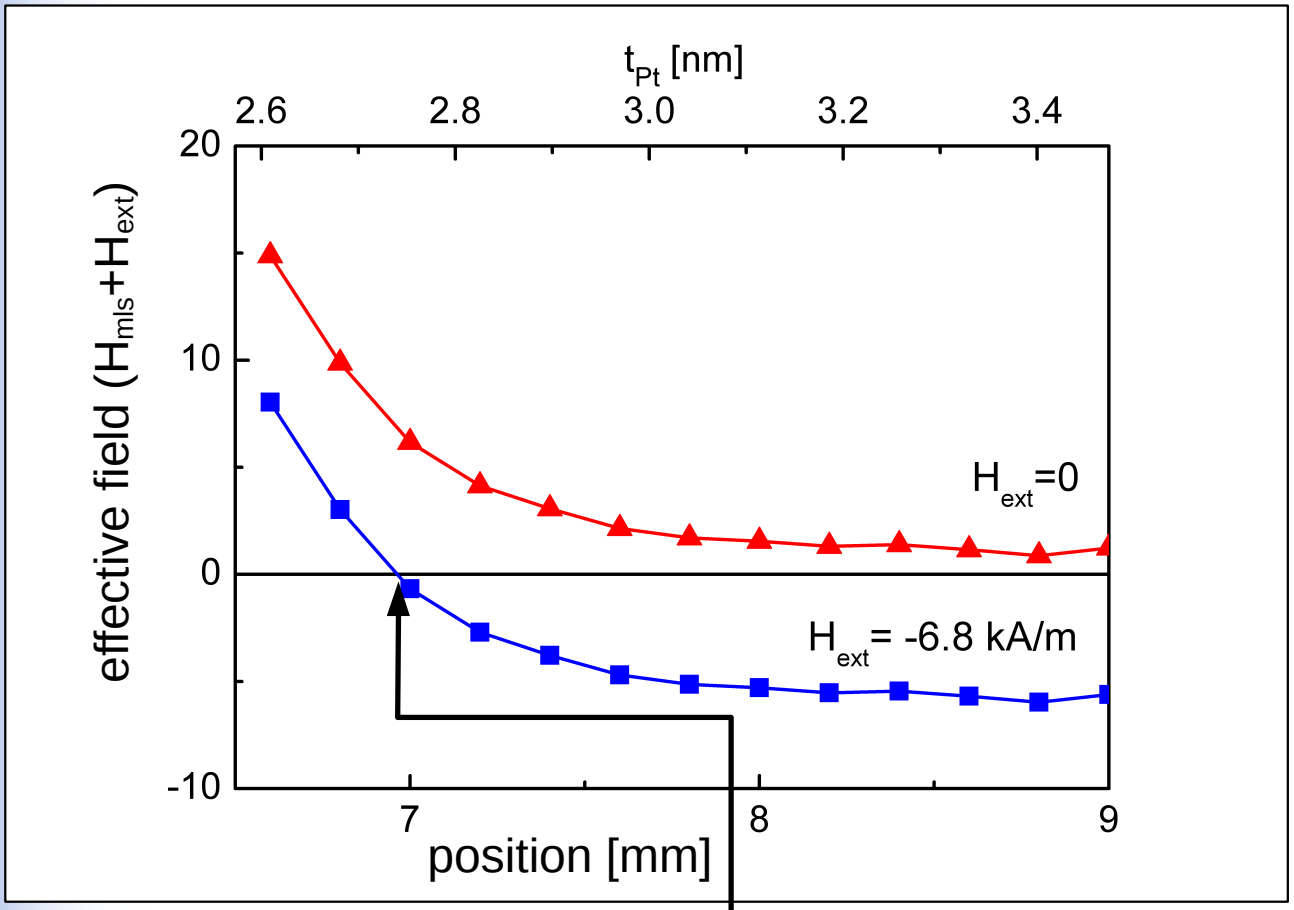


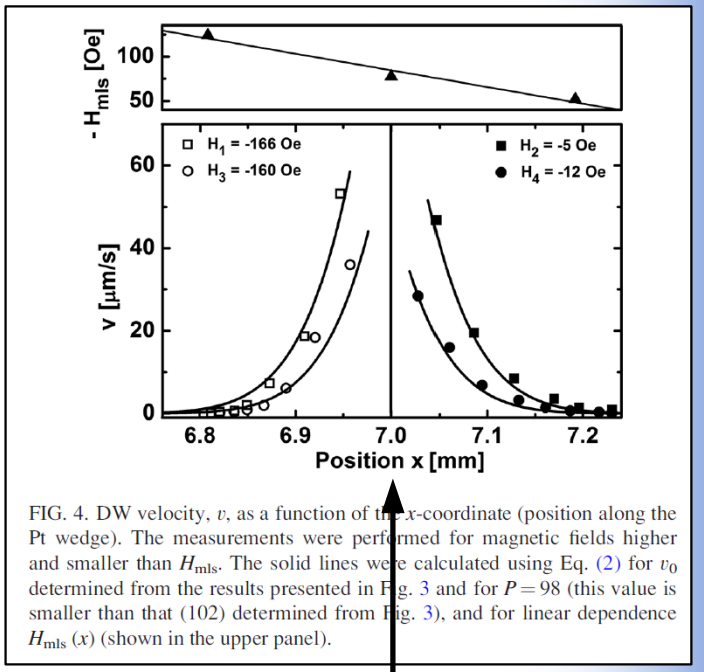


FIG. 4. DW velocity, $v$, as a function of the $x$-coordinate (position along the Pt wedge). The measurements were performed for magnetic fields higher and smaller than $H_{mls}$. The solid lines were calculated using Eq. (2) for $v_0$ determined from the results presented in Fig. 3 and for $P = 98$ (this value is smaller than that (102) determined from Fig. 3), and for linear dependence $H_{mls}(x)$ (shown in the upper panel).

equilibrium position (the effective field equal to zero) for $\boldsymbol{H_{ext}}$ **=-6.8 kA/m**

M. Matczak *et al.*, Appl. Phys. Lett. **107**, 012404 (2015)

# Co/Pt multilayers with coupling gradient

## Domain wall propagation in the presence of the gradient of ferromagnetic coupling

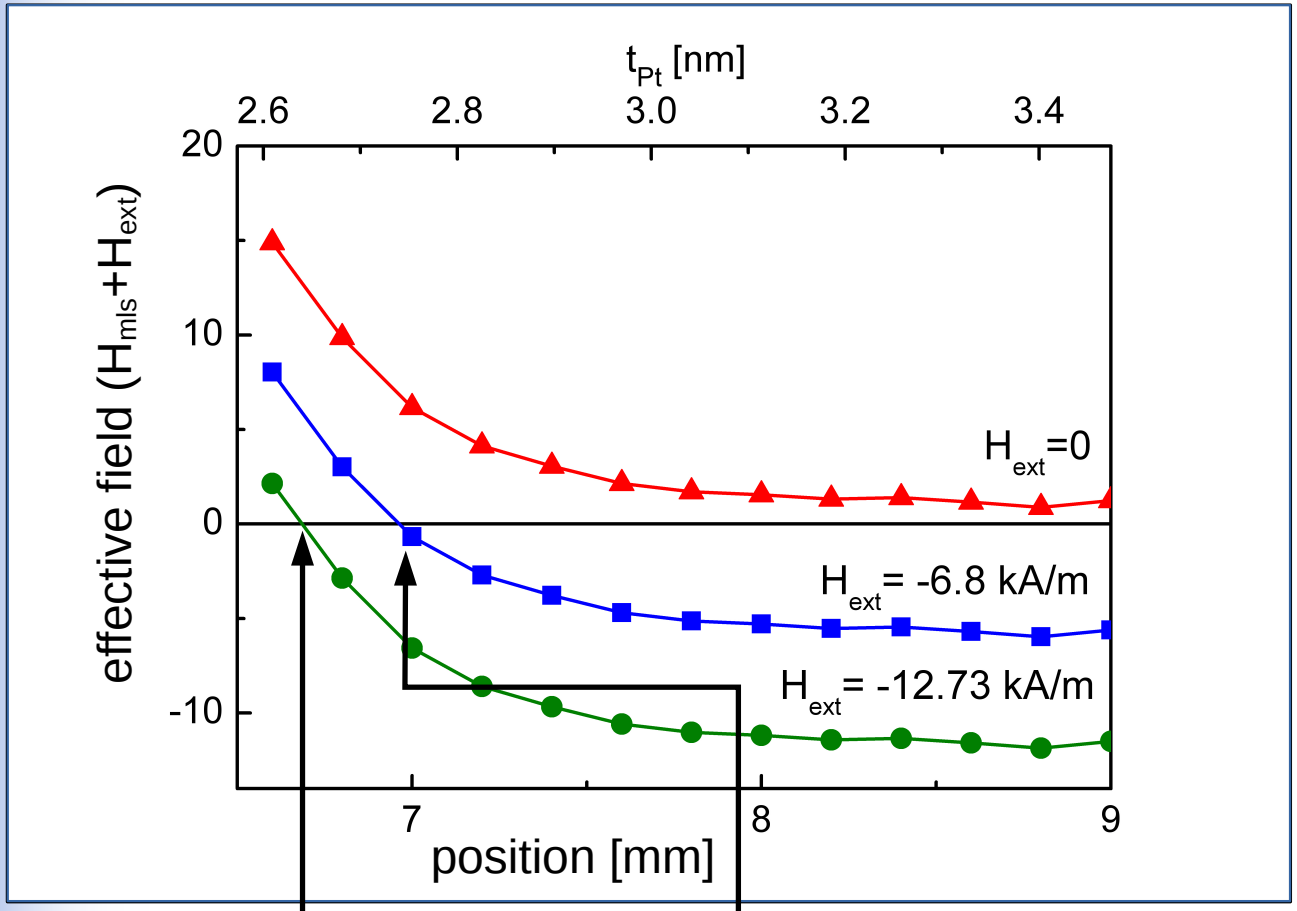


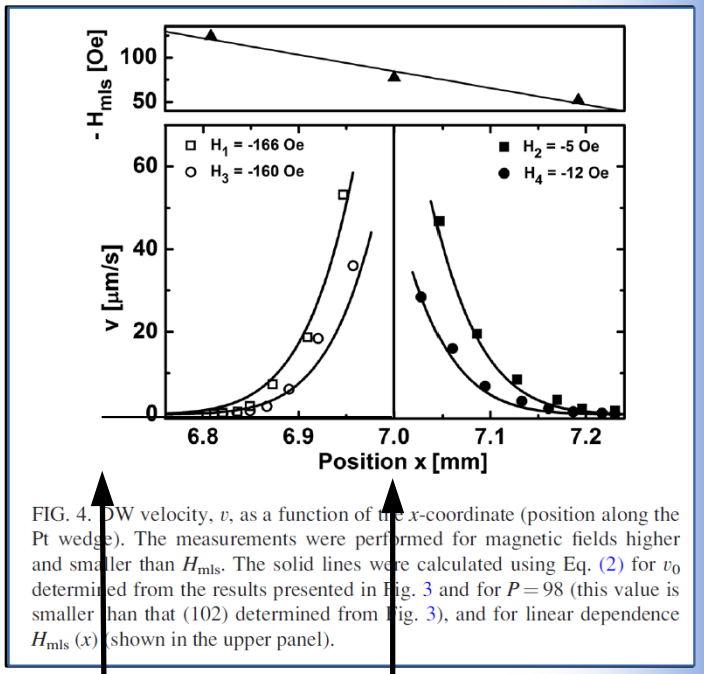


FIG. 4. DW velocity, $v$, as a function of the $x$-coordinate (position along the Pt wedge). The measurements were performed for magnetic fields higher and smaller than $H_{mls}$. The solid lines were calculated using Eq. (2) for $v_0$ determined from the results presented in Fig. 3 and for $P = 98$ (this value is smaller than that (102) determined from Fig. 3), and for linear dependence $H_{mls}(x)$ shown in the upper panel).

equilibrium position (the effective field equal to zero) for ***H*ext =-12.73 kA/m**

equilibrium position (the effective field equal to zero) for ***H*ext =-6.8 kA/m**

* -160 Oe

M. Matczak *et al.*, Appl. Phys. Lett. **107**, 012404 (2015)

Domain wall propagation in the presence of the gradient of ferromagnetic coupling

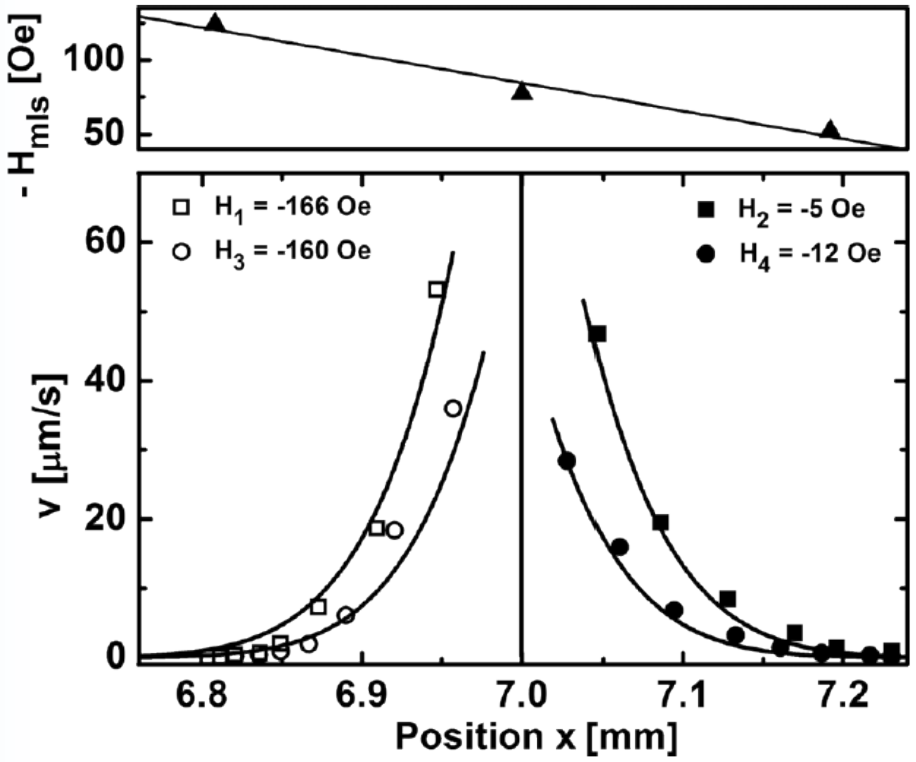


FIG. 4. DW velocity, $v$, as a function of the $x$-coordinate (position along the Pt wedge). The measurements were performed for magnetic fields higher and smaller than $H_{mls}$. The solid lines were calculated using Eq. (2) for $v_0$ determined from the results presented in Fig. 3 and for $P = 98$ (this value is smaller than that (102) determined from Fig. 3), and for linear dependence $H_{mls}(x)$ (shown in the upper panel).

The interlayer coupling between Co layers suppresses thermally activated creep in the magnetically soft layer

$$v = v_o \exp\left[-\frac{P}{(|H - H_{mls}|)^{(1/4)}}\right]$$

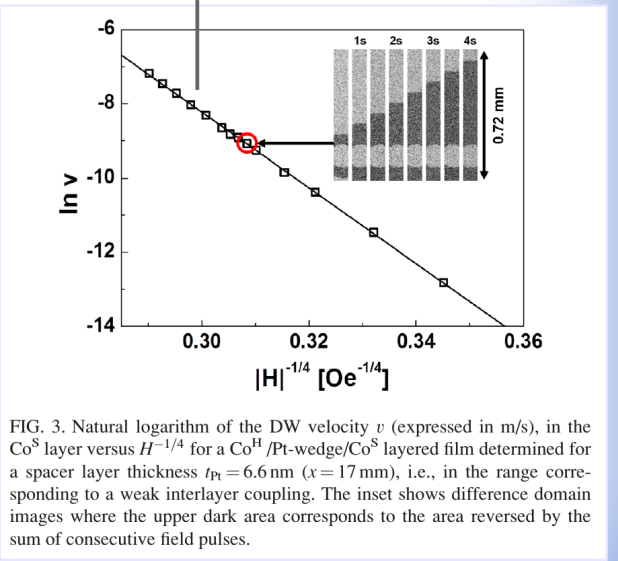


FIG. 3. Natural logarithm of the DW velocity $v$ (expressed in m/s), in the $Co^S$ layer versus $H^{-1/4}$ for a $Co^H$/Pt-wedge/$Co^S$ layered film determined for a spacer layer thickness $t_{Pt} = 6.6$ nm ($x = 17$ mm), i.e., in the range corresponding to a weak interlayer coupling. The inset shows difference domain images where the upper dark area corresponds to the area reversed by the sum of consecutive field pulses.



M. Matczak *et al.*, Appl. Phys. Lett. **107**, 012404 (2015)

# Co/Pt multilayers with coupling gradient


- prior to the measurements the sample was saturated in 1000 Oe
- within the area of high coupling gradients the position of the wall can be changed back and forth with the external field




M. Matczak *et al.*, Appl. Phys. Lett. **107**, 012404 (2015)

- Perpendicular magnetic anisotropy in Co based multilayers can be easily tailored with light ion bombardment
- The gradient of switching fields achieved this way can be use for domain walls positioning
- Control of domain walls position can be realized using the switching field gradients that are due to Co thickness gradients or using gradients of the interlayer coupling

The work was financed by the **National Science Centre Poland** under HARMONIA funding scheme for international research projects – decision No. DEC-2013/08/M/ST3/00960

# Measurement procedure

- We calculate the arithmetic difference between two images of the sample recorded for different magnetization configurations

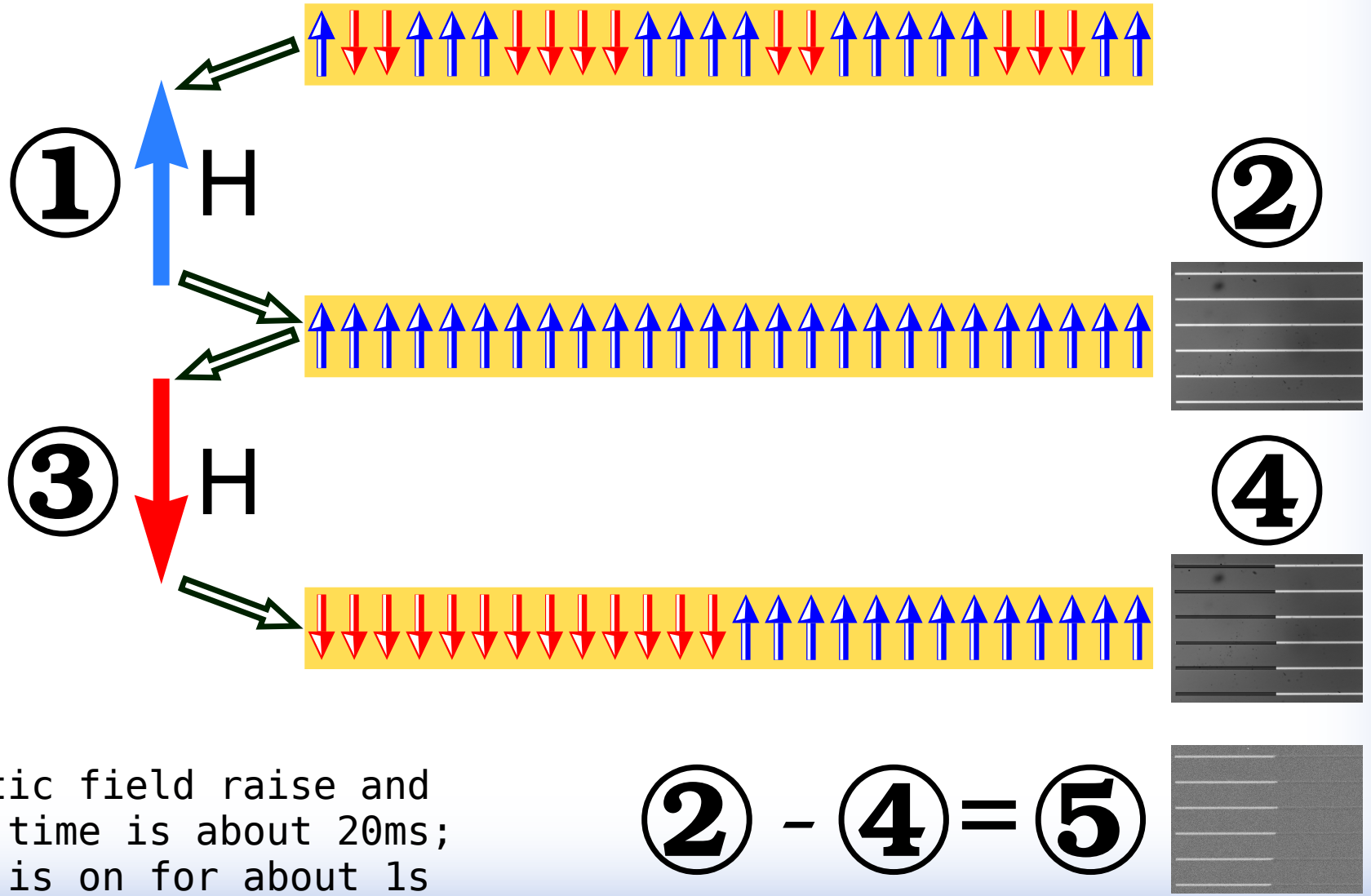


- Magnetic field raise and decay time is about 20ms; field is on for about 1s

# Au/Co/Au thin film - morphology

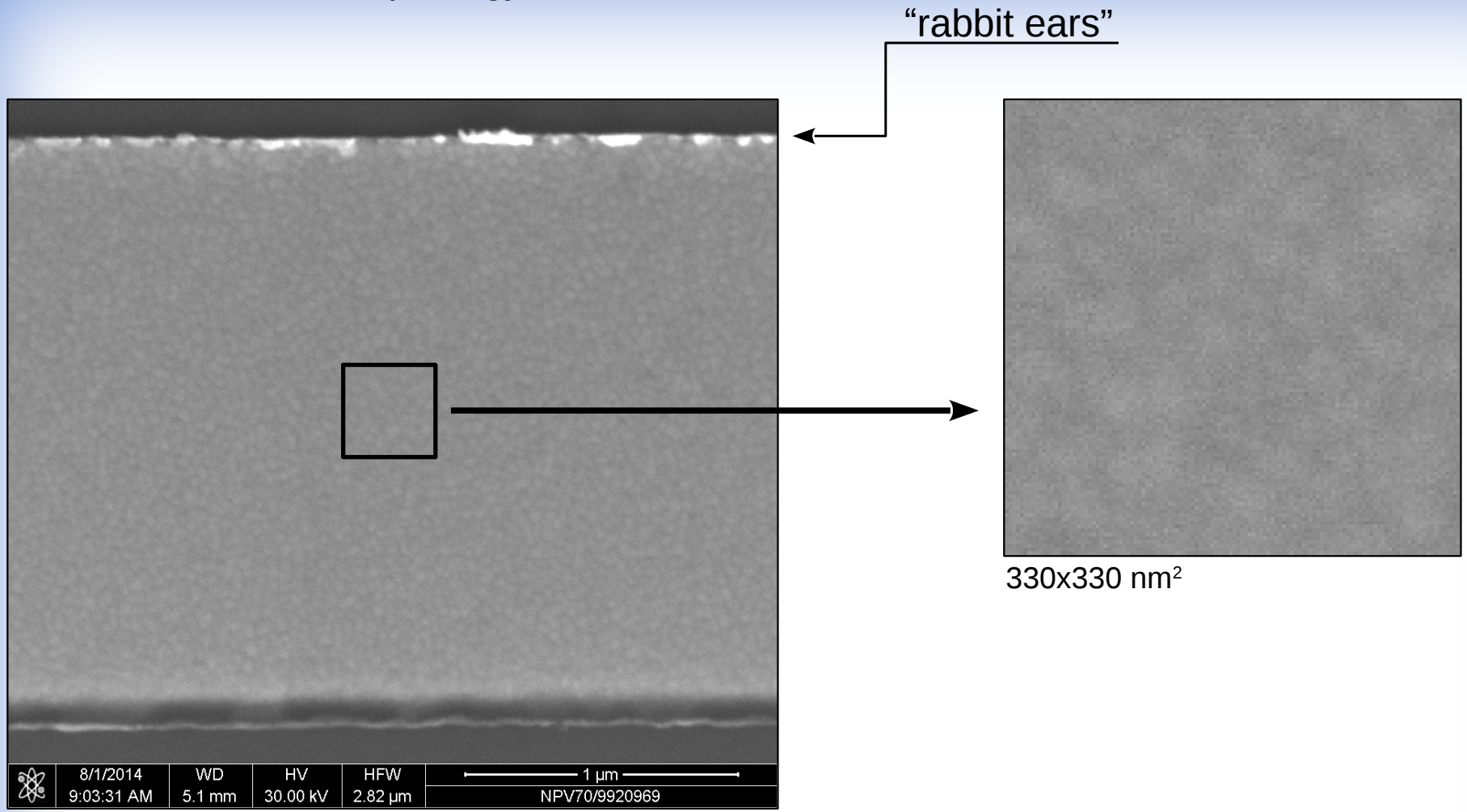


- grainy surface due to the structure of the Au buffer – grain boundaries may act as nucleation sites
- “rabbit ears” due to fabrication technique